

Development of a fast, robust and sensitive spectrophotometric assay for measuring hydroxycinnamic acid decarboxylation reactions

Larva, Mirna

Master's thesis / Diplomski rad

2023

Degree Grantor / Ustanova koja je dodijelila akademski / stručni stupanj: **University of Zagreb, Faculty of Food Technology and Biotechnology / Sveučilište u Zagrebu, Prehrambeno-biotehnološki fakultet**

Permanent link / Trajna poveznica: <https://urn.nsk.hr/urn:nbn:hr:159:342678>

Rights / Prava: [Attribution-NoDerivatives 4.0 International/Imenovanje-Bez prerada 4.0 međunarodna](#)

Download date / Datum preuzimanja: **2024-12-27**



Repository / Repozitorij:

[Repository of the Faculty of Food Technology and Biotechnology](#)



UNIVERSITY OF ZAGREB
FACULTY OF FOOD TECHNOLOGY AND BIOTECHNOLOGY

GRADUATE THESIS

Zagreb, May 2023

Mirna Larva

**DEVELOPMENT OF A FAST,
ROBUST AND SENSITIVE
SPECTROPHOTOMETRIC ASSAY
FOR MEASURING
HYDROXYCINNAMIC ACID
DECARBOXYLATION
REACTIONS**

This study was carried out at the Institute of Molecular Biotechnology at the Graz University of Technology under the supervision of Univ.-Prof. Dr.rer.nat. Robert Kourist, with the assistance of Daniel Kracher, Dipl.-Ing. Bakk.techn. PhD, and Anita Slavica, PhD, Full professor, Faculty of Food Technology and Biotechnology University of Zagreb.

ACKNOWLEDGEMENTS

First of all, I would like to express my special thanks to Univ.-Prof. Dr.rer.nat. Robert Kourist for allowing me to conduct scientific research under his mentorship at the Institute of Molecular Biotechnology at the Graz University of Technology.

I am incredibly grateful to my mentor Daniel Kracher, Dipl.-Ing. Bakk.techn PhD, for his continuous help and guidance through the experimental part of this scientific research. He enabled me to work independently and develop critical thinking under excellent guidance. But primarily, he was friend whom I could always ask for help. An especially important person on this scientific path was M.Sc Kamela Myrtollari, who trusted me with continuing her research. Her openness, immense help, and friendship further motivated me to conduct this research as successfully as possible.

Furthermore, I would like to thank Prof. dr. sc. Anita Slavica, PhD, for enabling this remarkable opportunity through endless support.

I want to thank all the members of the Institute for their constant help, advice, patience, and kindness, for being incredible friends and, above all, people. I'm incredibly thankful for meeting the best lab colleagues Ina Somvilla, Lucija Sović, Katarína Kavčiaková, Luigi Camerlenghi, Elske van der Pol, Marianna Karava, and Štela Galušić. Our coffee breaks, laughs, and amazing talks will stay with me forever.

Ogromna hvala mojim roditeljima, obitelji i prijateljima što su me podupirali kroz godinu dana života izvan vlastitog doma, na neopisivoj ljubavi i na tome što su me uvijek raširenih ruku čekali da se vratim. Bez vas ovo ništa ne bi imalo smisla!

Everyone who was part of or contributed to this thesis – thank you!

BASIC DOCUMENTATION CARD

Graduate Thesis

University of Zagreb
Faculty of Food Technology and Biotechnology
Department of Biochemical Engineering
Laboratory for Biochemical Engineering, Industrial Microbiology and Malting and Brewing Technology

Scientific area: Biotechnical Sciences

Scientific field: Biotechnology

Graduate university study programme: Molecular Biotechnology

DEVELOPMENT OF A FAST, ROBUST AND SENSITIVE SPECTROPHOTOMETRIC ASSAY
FOR MEASURING HYDROXYCINNAMIC ACID DECARBOXYLATION REACTIONS

Mirna Larva, univ. bacc. ing. biotechn. 0058208679

Abstract: Biocatalytic decarboxylation of bio-based hydroxycinnamic acids yields *p*-hydroxystyrene derivatives, which are important precursors of antioxidants, epoxy-coatings, adhesives and other polymeric materials. *Bacillus subtilis* phenolic acid decarboxylase (*Bs*PAD) is a cofactor-independent enzyme that catalyses the cleavage of carbon dioxide from hydroxycinnamic acids such as *p*-coumaric, caffeic, ferulic and sinapic acid with high catalytic efficiency. Current methods to kinetically characterise the decarboxylation reactions rely on HPLC, MS, GC or NMR, which require extensive sample work-up while measuring only endpoint concentrations. In this work, we use a fast, robust and sensitive spectrophotometric assay that allows following decarboxylation reactions in real-time while avoiding product extraction. Absorption spectra of the pure reaction products were recorded after verifying the completeness of the reactions by TLC and NMR analyses. An optimized assay procedure was used to measure the kinetic constants (K_M and V_{max} values) of *Bs*PAD for three substrates, which indicates the broad applicability of the assay.

Keywords: *p*-hydroxycinnamic acids, phenolic acid decarboxylase, UV-VIS spectrophotometric assay

Thesis contains: 71 pages, 17 figures, 10 tables, 57 references, 0 supplements

Original in: English

Graduate Thesis in printed and electronic (pdf format) form is deposited in: The Library of the Faculty of Food Technology and Biotechnology, Kačićeva 23, Zagreb.

Mentor: Anita Slavica, PhD, Full Professor

Co-mentor: Robert Kourist, Univ.-Prof. Dr.rer.nat., Institute of Molecular Biotechnology, Graz University of Technology

Technical support and assistance: Daniel Kracher, Dipl.-Ing. Bakk.techn. PhD

Reviewers:

1. Renata, Teparić, PhD, Full professor
2. Anita, Slavica, PhD, Full professor
3. Robert, Kourist, Univ.-Prof. Dr.rer.nat.
4. Blaženka, Kos, PhD, Full professor

Thesis defended: 11th of May, 2023

TEMELJNA DOKUMENTACIJSKA KARTICA

Diplomski rad

Sveučilište u Zagrebu

Prehrambeno-biotehnološki fakultet

Zavod za biokemijsko inženjerstvo

Laboratorij za biokemijsko inženjerstvo, industrijsku mikrobiologiju i tehnologiju piva i slada

Znanstveno područje: Biotehničke znanosti

Znanstveno polje: Biotehnologija

Diplomski sveučilišni studij: Molekularna biotehnologija

RAZVOJ BRZE, ROBUSNE I OSJETLJIVE SPEKTROFOTOMETRIJSKE METODE ZA MJERENJE
REAKCIJA DEKARBOKSILACIJA HIDROKSICIMETNIH KISELINA

Mirna Larva, univ. bacc. ing. biotechn. 0058208679

Sažetak: Biokatalitičkom dekarboksilacijom prirodnih hidroksicimetnih kiselina dobiju se derivati *p*-hidroksistirena, koji su važni prekursori u proizvodnji antioksidansa, epoksi premaza, adheziva i drugih polimernih materijala. Dekarboksilaza fenolnih kiselina iz bakterije *Bacillus subtilis* (*BsPAD*) je enzim neovisan o kofaktoru, koji katalizira izdvajanje ugljičnog dioksida iz *p*-hidroksicimetnih kiselina poput *p*-kumarinske, kofeinske, ferulinske i sinapinske kiseline uz visoku katalitičku učinkovitost. Metode koje se koriste za kinetičku karakterizaciju reakcija dekarboksilacije se temelje na korištenju HPLC, MS, GC ili NMR, i zahtijevaju opsežnu pripremu uzoraka, a njima se određuje samo krajnja koncentracija produkata ovih reakcija. U ovom diplomskom radu razvijena je brza, robusna i osjetljiva spektrofotometrijska metoda kojom se reakcija dekarboksilacije prati u realnom vremenu i kod koje nije potrebna ekstrakcija dobivenih produkata. Apsorpcijski spektri produkata snimljeni su nakon potvrde o kompletnoj dekarboksilaciji supstrata i to dvjema metodama - TLC i NMR. Optimizirana metoda korištena je za određivanje kinetičkih konstanti (K_M i V_{max}) za tri supstrata *BsPAD*, što ukazuje na široku primjenu ove razvijene metode.

Ključne riječi: *p*-hidroksicimetne kiseline, dekarboksilaza fenolne kiseline, UV-VIS spektrofotometrijska metoda

Rad sadrži: 71 stranica, 17 slika, 10 tablica, 57 literaturnih navoda, 0 priloga

Jezik izvornika: engleski

Rad je u tiskanom i elektroničkom (pdf format) obliku pohranjen u: Knjižnica Prehrambeno-biotehnološkog fakulteta, Kačićeva 23, Zagreb

Mentor: prof. dr. sc. Anita Slavica

Komentor: Univ.-Prof. Dipl.-Ing Robert Kourist, Institute of Molecular Biotechnology, Graz University of Technology

Pomoć pri izradi: Daniel Kracher, Dipl.-Ing., Bakk. techn. Dr. Sc.

Stručno povjerenstvo za ocjenu i obranu:

1. prof. dr. sc. Renata Teparčić
2. prof. dr. sc. Anita Slavica
3. Univ.-Prof. Dr.rer.nat. Robert Kourist
4. prof. dr. sc. Blaženka Kos

Datum obrane: 11. svibanj 2023.

TABLE OF CONTENT

1. INTRODUCTION	1
2. LITERATURE REVIEW	3
2.1 PLANT PRIMARY AND SECONDARY METABOLITES	3
2.2. CLASSIFICATION OF PLANT SECONDARY METABOLITES	4
2.2.1. Phenolic compounds	4
2.3. PHENOLIC ACID DECARBOXYLASE FROM <i>Bacillus subtilis</i>	9
2.4. COMMONLY USED METHODS FOR DETERMINATION OF THE <i>p</i>- HYDROXYCINNAMIC ACIDS AND <i>p</i>-HYDROXYSTYRENE DERIVATES	12
2.4.1. Thin-Layer Chromatography (TLC)	12
2.4.2. Gas Chromatography (GC)	12
2.4.3. High-Performance Liquid Chromatography (HPLC)	13
2.5. UV-VIS SPECTROSCOPY	15
3. EXPERIMENTAL PART	18
3.1. MATERIALS	18
3.1.1. Cell cultures	18
3.1.2. Media used for the cultivation of <i>E. coli</i> BL21 (DE3) strain.....	18
3.1.3. The column used for protein purification by affinity chromatography	18
3.1.4. Membrane used for imidazole removal.....	18
3.1.5. Concentrator tube used for buffer exchange after protein purification	19
3.1.6. Kit used for protein quantification	19
3.1.7. Well plates used in this research	19
3.1.8. Aluminium plates used for thin-layer chromatography (TLC)	19
3.2. METHODS	21
3.2.1. Expression and purification of recombinant phenolic acid decarboxylases from <i>Bacillus subtilis</i> (<i>BsPAD_wt</i> and <i>BsPAD_I85A</i>)	21
3.2.2. Purification of expressed <i>BsPAD_wt</i> and <i>BsPAD_I85A</i>	22
3.2.3. Determination of phenolic acid decarboxylase concentration	23
3.2.4. Sodium dodecyl-sulfate polyacrylamide gel electrophoresis (SDS-PAGE)	24
3.2.5. Reaction conditions for complete substrates conversion for the TLC and ¹ H NMR analysis ..	24
3.2.6. HPLC-UV analysis	26
3.2.7. Spectrophotometric assay for the determination of <i>BsPAD</i> activity.....	29
4. RESULTS AND DISCUSSION	31

4.1. EXPRESSION AND PURIFICATION OF RECOMBINANT PHENOLIC ACID DECARBOXYLASE FROM <i>Bacillus subtilis</i> (<i>BsPAD_wt</i> and <i>BsPAD_I85A</i>)	32
4.1.1. Protein expression of <i>BsPAD</i> wild type (<i>BsPAD_wt</i>) and <i>BsPAD</i> mutant (<i>BsPAD_I85A</i>).....	32
4.2.1. TLC confirmation of substrates conversion.....	33
4.3. DEVELOPMENT OF AN UV-VIS SPECTROPHOTOMETRIC ASSAY FOR THE ACTIVITY AND KINTEIC MEASUREMENTS OF PHENOLIC ACID DECARBOXYLASE FROM <i>Bacillus subtilis</i>	40
4.3.1. UV-VIS absorbance spectra of substrates (<i>p</i> -CUA, CAA, FA and SA) and decarboxylated products (4-VP, 4-VC, 4-VG and 4-VS).....	40
4.3.2. Comparison of specific activity of <i>BsPAD_wt</i> and <i>BsPAD_I85A</i> followed by the HPLC and UV-VIS spectroscopy	46
4.3.3. Determination of the kinetic constants (K_M and V_{max} values) of <i>BsPAD_wt</i> for <i>p</i> -CUA, CAA and FA.....	51
4.3.4. PAD activity assay protocol.....	54
5. CONCLUSIONS	56
6. LITERATURE	58

1. INTRODUCTION

Higher plants synthesize an immense amount of chemicals of various structures and classes, of which more than 200,000 individual chemical entities have been isolated and identified (Lattanzio, 2013). These substances are further classified as primary and secondary metabolites. Primary metabolites are essential compounds used by all plants for growth, development and reproduction. Secondary metabolites are structurally and chemically much more diverse and refer to compounds that are not directly required for primary respiratory or photosynthetic metabolism but are thought to be necessary as a competitive advantage for plant survival in the environment (Wu and Chappell, 2008). Specialized cells in organisms synthesize *via* different metabolic pathways tens of thousands of these secondary compounds that can effectively respond to biotic and abiotic stressors. Phenolic compounds are the most abundant secondary metabolites in the plant kingdom (Lattanzio, 2013). A subcategory of phenolic compounds is hydroxycinnamic acids, naturally occurring molecules that contribute to plant rigidity by linking the complex lignin polymer to plant cell wall hemicelluloses and cellulose. Simple phenolic acids such as *p*-coumaric, caffeic, ferulic, and sinapic acids can be covalently attached to the plant cell wall or freely diffuse in the cytoplasm (Landete et al., 2010). Decarboxylation is a common enzymatic transformation of phenolic acids that results in vinyl phenol derivatives. This enzymatic conversion is thought to be used by bacteria as a mechanism to reduce the accumulation of toxic phenolic acids (Tran et al., 2008), and it is also responsible for the formation of phenolic acid-derived phenols acting as flavouring compounds in alcoholic beverages (Vanbeneden et al., 2008). Several organisms have evolved the ability to transform these potentially toxic phenolic acids (Zaldivar et al., 1999) *via* various metabolic pathways (Rosazza et al., 1995), including phenolic acid decarboxylase (PAD) from *Bacillus subtilis* (*BsPAD*). *BsPAD* is cofactor independent enzyme that catalyzes the non-oxidative decarboxylation of phenolic acids to their corresponding *p*-vinyl derivatives (Priefert et al., 2001). The enzymatic decarboxylation of these organic molecules derived from renewable feedstock has received much attention since these processes can lead to sustainable routes to produce precursors for commodity chemicals (Hermann et al., 2007) and high-value products for the flavour and fragrance industry (Vanbeneden et al., 2008; Serra et al., 2005). Because lignin is a renewable resource, PADs may also be suitable biocatalysts for the production of styrene derivatives as polymer industry precursors (Jung et al., 2013). *BsPAD* wild type (*BsPAD_wt*)

catalyzes the conversion of *p*-coumaric, caffeic and ferulic acid into the volatile compounds 4-vinyl phenol, 4-vinyl catechol and 4-vinyl guaiacol. A recently introduced variant (*Bs*PAD_I85A) also catalyzes the conversion of sinapic acid to 4-vinyl syringol (Morley et al., 2013). 4-Vinyl guaiacol, a product of mentioned enzymatic transformation, is considered one of the precursors to vanillin production (Koseki et al., 1996), which is commonly used flavoring compound in foods, beverages, perfumes, and pharmaceuticals (Zheng et al., 2007). 4-Vinyl guaiacol is 40 times more valuable than ferulic acid and can be biotransformed into acetovanillone, ethyl guaiacol, and vanillin (Mathew et al., 2007). Furthermore, PAD-catalyzed decarboxylation of *p*-coumaric and ferulic results in the formation of vinyl phenol and 4-vinyl guaiacol, which are food additives and have been approved as flavoring agents by regulatory agencies (Anonymous 1, 2001). Although PADs were discovered several decades ago, their biochemical characterisation largely relies on complex and time-consuming methods such as gas chromatography (GC; Mojzer et al., 2016), high-performance liquid chromatography (HPLC; Hu et al., 2014; Landete et al., 2010) or even mass spectrometry (MS; Hu et al., 2015). While the UV-absorbance of hydroxycinnamate substrates has been used in some cases, the overlapping UV absorbance of the hydroxycinnamates with their corresponding decarboxylation products has been neglected (Williamson et al., 2020; Noda et al., 2015; Cavin et al., 1998; Cavin et al., 1997; Cavin et al., 1993). Current methods to kinetically characterize and measure the activity of *PAD*-catalyzed decarboxylation reactions require specialized equipment and extensive sample work-up, therefore do not provide the possibility for high-throughput measurements. Spectral shifts in the UV range caused by substrate decarboxylation have been used to screen a PAD library generated by site-saturation mutagenesis (Morley et al., 2013) in addition to these mentioned commonly used methods. However, the overlapping UV absorbance of hydroxycinnamates and their corresponding derivatives complicate kinetic measurements. This study aimed to develop a fast, robust and sensitive spectrophotometric assay that allows following *Bs*PAD decarboxylation reactions in real-time while avoiding product extraction. In the current research, *Bs*PAD_wt and *Bs*PAD_I85A were expressed in *E. coli* BL21 (DE3), purified, and their substrate conversion was shown by thin-layer chromatography (TLC) and ¹H NMR. *Bs*PAD_wt and *Bs*PAD_I85A activity results obtained by spectrophotometric assay were proven with HPLC-UV analysis.

2. LITERATURE REVIEW

2.1 PLANT PRIMARY AND SECONDARY METABOLITES

Metabolism implies synthesizing and breaking down chemical compounds through a series of chemical reactions catalyzed by enzymes in living organisms. Plant metabolism is usually divided into two categories - primary and secondary metabolism. The primary metabolism includes synthesizing or consuming chemical substances such as amino acids, nucleic acids, fatty acids and sugars. These primary metabolites play a vital role in cell metabolism because cells use them to build cofactors, precursors and other biopolymers that enable growth and reproduction. Primary metabolism includes all biochemical processes an organism must carry out to survive, which is why they are of essential importance (Maeda, 2019).

Secondary metabolites are a class of organic molecules produced by plants and microorganisms that do not directly contribute to growth or development and are typically produced by only one kind of organism or even just one strain. These compounds are not essential to sustain an organism's survival or growth, but they give it a selective advantage when interacting with the environment (Ncube et al., 2017). Each organism contains particular set of enzymes in a specific tissue, resulting in the specificity of the metabolic process and contributing to the alteration of the fundamental biosynthetic pathway and the formation of various metabolites. To date, the majority of secondary metabolic pathways in plants have not yet been fully mapped and characterised (Zhao et al., 2013; Pichersky and Gang, 2000). Because secondary metabolites have evolved opportunistically, each imparting its unique advantage, they do not have a common, universal purpose. There is a widespread presence of multifunctional enzymes in the plant kingdom. However, the synthesis of secondary compounds is not only determined by enzyme specificity, but it is also essential to consider substrate availability and compartmentation (Schwab, 2003).

A plant's natural habitat is filled with various biotic and abiotic stress factors, and the formation of secondary metabolites results from physiological regulation in reaction to environmental stress. Plants are surrounded by a large number of potential enemies (bacteria, molds, viruses, stress). These elicitors are substances of biological or non-biological origin that, in

contact with plant cells, cause physiological or morphological changes that include increased synthesis or *de novo* synthesis of secondary metabolites. Since plants are immobile, receiving stress signals and translating them into useful responses are essential for plant survival and adaptability (Bartwal et al., 2012).

2.2. CLASSIFICATION OF PLANT SECONDARY METABOLITES

Secondary metabolites are categorized based on their chemical structure, solubility, pathway by which they are synthesized or their composition. The primary classification includes three main groups:

1. Terpenoids (limonoids, saponin and pinene)
2. Alkaloids (nicotine, morphine, cocaine, caffeine and glucosinolates)
3. Phenolic compounds (flavonoids, anthocyanidins, salicylic acid and lignin)

The most prevalent and structurally diverse family of secondary metabolites found in many plants are terpenoids, sometimes referred to as isoprenoids. They constitute the most important class of active chemicals in plants, with more than 60 000 known structures (Agatonovic-Kustrin and Morton, 2018).

Alkaloids are a group of nitrogen-containing secondary metabolites derived from amino acids. Structurally, they differ from other secondary metabolites and thus lack a standardized classification. Numerous organisms, including bacteria, fungi, mammals and plants, synthesize alkaloids, most of which are toxic to other organisms. Due to their advantageous biological features, alkaloids have been extensively explored and divided into categories based on their biosynthetic precursor and heterocyclic ring system (Mondal, 2019).

2.2.1. Phenolic compounds

Phenolic compounds are the most widely distributed secondary metabolites naturally found throughout the plant kingdom. While some phenolic compounds are ubiquitous in plants, others

can be found in only specific plant groups, organs or even at different development stages (Iannucci et al., 2013). For example, non-vascular land plants (bryophytes) lack developed physical barriers but regularly synthesize a diverse range of phenolics, such as flavonoids, enabling them to tolerate unfavorable abiotic and biotic stresses (Dziwak et al., 2022). On the other hand, the whole spectrum of phenolic compounds is only found in vascular plants that produce thousands of distinct phenolics already described. They are represented by at least 10 000 different identified compounds that include one or more aromatic rings with one or more hydroxyl groups connected to them (Li et al., 2014). Phenolic compounds are synthesized either *via* the polyketide or shikimic acid pathway, which account for around 40 % of the organic carbon circulating in the biosphere (Lattanzio, 2013). They exhibit a wide range of structural variations, including hydroxycinnamic acids (caffeic acid, vanillin, gallic acid), polyphenols such as flavonoids and polymers derived from these building blocks.

Phenolic compounds as secondary metabolites also show a variety of beneficial human health-related abilities. Anthocyanins, for instance, can be found either in ripe fruits and plants acting as attractants or in young leaves with a deterrent effect against herbivore insects (Gloud, 2010). Phenolic compounds are free radical scavengers and chelators having an antioxidant activity that is particularly effective against hydroxyl and peroxy radicals, superoxide anions, and peroxy nitrates (Lall et al., 2015). In humans, once consumed, they show antioxidant properties (Merecz-Sadowska et al., 2021), can be used as supplementary and nutraceutical treatment for diabetes and related disorders (Rasouli et al., 2017), and exhibit therapeutic antiplatelet, vasodilatory and anti-inflammatory effects against cardiovascular pathologies (Alotaibi et al., 2021). Two phenolic compounds even showed activity against SARS-coronavirus protease. These compounds became a crucial target for drug development (Lin et al., 2005), which served as a base for further research during the COVID-19 pandemic (Chen et al., 2023; Jo et al., 2020). Phenolic compounds can be divided into (a) phenolic acids such as benzoic and cinnamic acids and their hydroxylated derivatives, and (b) polyphenols such as flavonoids, stilbenes and coumarins, lignin and tannins.

More than 8000 different organic molecules fall under the classification of phenolic acids, containing a phenol ring with at least one hydroxyl group (Robbins, 2003). Simple phenolic acids are the most prevalent among the thousands of compounds involved in ecological interactions in

soils, and many of them are referred to as plant allelochemicals, which are one of the mechanisms by which a plant survives in nature and reduces competition from nearby plants (Marchiosi et al., 2020). Many of them, including hydroxycinnamic acids, are intermediates or structural components of the plant cell wall (de Oliveira et al. 2015).

Cinnamic acid is suggested precursor to *p*-hydroxycinnamic acids (Bourgaud et al., 2006) that have been known for centuries as significant and one of the main classes of phenolic compounds found in nature that possess multiple biological properties (Alam et al., 2016). This family includes several simple phenolic compounds such as ferulic acid, *p*-coumaric acid, caffeic acid and sinapic acid. A plant produced *p*-hydroxycinnamic acids and their corresponding derivatives give them resistance by joining hemicelluloses and lignin in the plant cell wall (ferulic and *p*-coumaric acid), or protect them from insects and oxidative stress, as in the case of sinapoyl malate and chlorogenic acid. Also, they are valuable and particularly appealing compounds in the pharmaceutical and cosmetic industries because they can operate as high-value precursors of anti-UV compounds, antioxidants, vanillin, monomers and polymer additives (Flourat et al., 2020). Plants synthesize hydroxycinnamic acids *via* an essential primary and secondary metabolism pathway. The Shikimate biosynthesis pathway leads to the synthesis of tyrosine and phenylalanine, significant aromatic amino acids, by converting simple primary metabolites, phosphoenolpyruvate and erythrose 4-phosphate, in higher plants. A series of enzymatic reactions follow the phenylalanine ammonia-lyase (PAL) catalyzed reaction to produce hydroxycinnamate from previously mentioned aromatic amino acids. PAL catalyzes the deamination of phenylalanine or tyrosine to produce the C3-C6 unit, which serves as the core structural component of phenylpropanoids, linking amino acids to the hydroxycinnamic acids and their activated forms (El-Seedi et al., 2012). Phenylpropanoids may function as phytoalexins in some plant species because the stimulation of PAL expression is frequently seen as a component of the reactions of plants to encroaching microbes (Liang et al., 1989). It has been established that every studied plant possesses several copies of genes that encode for the PAL, each of which is differentially expressed. In plants, the conversion of tyrosine into 4-hydroxycinnamic acid (also known as *p*-coumaric acid) is also catalyzed by tyrosine ammonia-lyase (TAL). *p*-Coumaric acid is also a precursor in the biosynthesis of ferulic, caffeic or sinapic acid. Chemical decarboxylation of *p*-hydroxycinnamic acids requires expensive base catalysis with microwave heating (Ben-Bassat et al., 2005) or harsh reaction conditions such as high temperature and pressure. That is why

enzymatic decarboxylation, which employs mild temperature and generates little waste, is a potential alternative for the *p*-hydroxystyrene production. Enzymes that catalyze the decarboxylation may potentially be used to convert phenolic acids derived from renewable sources into styrene derivatives for the polymer industry (Lee et al., 1998).

2.2.1.1. Simple phenolic acids

Coumaric acid is a naturally occurring hydroxy derivate of cinnamic acid, which has three distinct isomers (*ortho*-, *meta*-, and *para*-). The most prevalent type, *p*-coumaric acid (4-hydroxycinnamic acid, C₉H₈O₃; figure 1. a) (Boz, 2015), is found in the cell walls of numerous vegetables, fruits and seeds such as broccoli, eggplant, tomato, carrot, blueberries, peanuts and others. Due to its role in the defense against bacterial pathogens (Li et al., 2009), chemoprotective (Torres and Rosazza 2001) and antioxidative (Kilic, 2013) properties, *p*-coumaric acid is of high economic interest. Decarboxylation of *p*-coumaric acid results in the formation of 4-vinyl phenol.

Caffeic acid (3,4-dihydroxy cinnamic acid; C₉H₈O₄, figure 1. b) is found in many plant products, including coffee, fruits, wine, olive oil, and legumes (Stojković et al., 2013). Caffeic acid has been linked to several plant interactions, including allelopathy between plants and microorganisms (Batish et al., 2008), but it also greatly influences human health. Caffeic acid can inhibit the biosynthesis of leukotrienes, which are involved in allergic responses, asthma, and other immune-regulatory illnesses (Koshihara, 1984). Several of its ester derivatives may inhibit the development of colon cancer (Olthof, 2001).

The cell walls of various plants contain high concentrations of ferulic acid (4-hydroxy-3-methoxy cinnamic acid, C₁₀H₁₀O₄, figure 1. c; Abraham et al., 2007). The molecule is primarily present in the *trans* form and is esterified with hemicelluloses and arabinoxylans. It is found in the leaves and seeds of many plants, especially in grains such as wheat and oats. Ferulic acid contains a single *para*-substituted hydroxyl group connected to a highly conjugated side chain, which allows the phenoxy radical of ferulic acid to be delocalized and stabilized throughout the entire molecule (Graf, 1992). In plant cell walls, ferulic acid plays a crucial role in pathogen defense (Ren et al., 2020; Blokker et al., 2006), the response to abiotic stress (Novaković et al., 2018) and is toxic to herbivorous insects (Yang et al., 2017).

Sinapic acid (3,5-dimethoxy-4-hydroxycinnamic acid; C₁₁H₁₂O₅), also called sinapinic acid, has two methoxy groups attached to the phenyl ring (figure 1. d). Although it can occur in the form of sinapate esters, like other hydroxycinnamic acids, it can also be found in a free form. Sinapic acid and some of its derivatives can be potentially applied as preservatives in foods, cosmetics, and the pharmaceutical industry (Nićiforović, 2013).

p-Coumaric, ferulic, and caffeic acid also link the complex lignin polymer to the cellulose and hemicelluloses in plant cell walls, where they are typically esterified with tartaric acid (El-Seedi et al., 2018). Many microorganisms can metabolize free phenolic acids to 4-vinyl derivatives using specific phenolic acid decarboxylase enzymes. The decarboxylated reaction products, 4-hydroxy styrenes, can inhibit the growth of a wide variety of Gram-negative bacteria, including pathogens and food spoilage flora (Cavin et al., 1998). They are valuable compounds that can be used as flavor enhancers in the production of chewing gums, in bakery and meat products, desserts and confectionery and in alcoholic beverages. Ferulic acid-derived 4-vinyl guaiacol is a precursor for the synthesis of fragrance compounds (van Beek and Priest, 2000) or biodegradable polymers (Zago et al., 2016). The supply of 4-vinyl derivatives such as 4-vinyl phenol, 4-vinyl guaiacol and others from natural sources is insufficient to meet industrial demand (Bernini et al., 2007). Currently, in industry, 4-vinyl phenol is produced by dehydrogenating 4-ethylphenol over an expensive catalyst (chromia-alumina) and at a high temperature (600 °C) with a low yield (15 %). In addition, 4-ethylphenol is derived from nonrenewable fossil materials (Qu et al., 2013).

Caffeic acid is an abundant catechol-containing natural aromatic compound that can be converted to 4-vinyl catechol (Takeshima et al., 2018). It can be used for synthesizing catechol-containing polymers used as functional coating materials (Nishimori et al., 2020) due to their strong binding to a large variety of surfaces like gold, silicon and metal oxides (Leibig et al., 2016). Canolol, also known as 4-vinyl syringol, is a main phenolic compound in canola (Krygier et al., 1982), and it is identified as the decarboxylation product of sinapic acid (Galano, 2011). Vinyl syringol is recognized as a radical scavenger (Koski et al., 2003), and it is a potential precursor for the production of the biodegradable polymer polyvinylsyringol (PVS) (Morley et al., 2013).

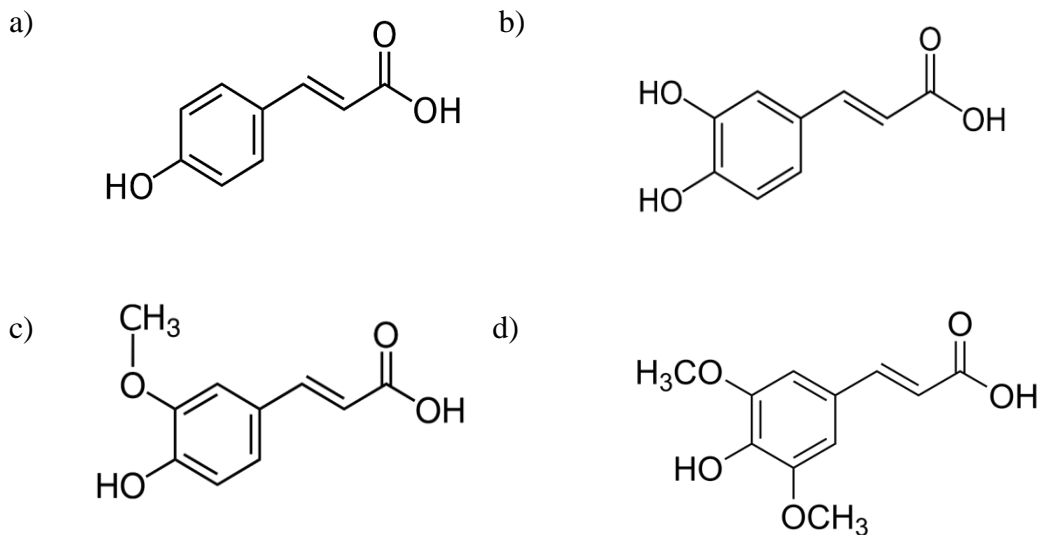


Figure 1. Molecular structures of simple phenolic acids used in this research. a) *p*-coumaric (*p*-CUA), b) caffeic acid (CAA), c) ferulic acid (FA) and d) sinapic acid (SA)

2.3. PHENOLIC ACID DECARBOXYLASE FROM *Bacillus subtilis*

In plant-soil systems, when lignocellulose is broken down enzymatically by bacteria and fungi, cinnamic acid derivatives such as *p*-coumaric, ferulic, caffeic and sinapic acids are released (Jung et al., 2013). Enzymatic decarboxylation by bacterial decarboxylases is a potential defense mechanism that prevents the accumulation of phenolic acids, which show toxicity towards the bacteria. In response to toxic stress caused by previously mentioned free phenolic acids, some microorganisms such as *Bacillus pumilus* and *Lactobacillus plantarum* degrade cinnamic acid derivatives through non-oxidative decarboxylation (Rodriguez et al., 2008; Cavin et al., 1998; Degraasi et al., 1995). Phenolic acid decarboxylase (PAD) catalyzes the nonoxidative decarboxylation of *p*-hydroxycinnamic acids to their corresponding *p*-hydroxystyrenes. According to their substrate specificity, PAD-type enzymes can be classified as ferulic acid (FAD) or *p*-coumaric acid decarboxylase (PDC). Despite having a 66 % amino acid sequence identity, PADs from different origins have different structures, physicochemical properties and substrate specificities.

The screening of a genomic library of the Gram-positive bacterium *Bacillus subtilis* led to the discovery and characterization of the first phenolic acid decarboxylase (*BsPAD*) that could decarboxylate *p*-coumaric, caffeic and ferulic acid to yield *para*-hydroxy styrene derivatives (figure 2) (Cavin et al, 1998). *BsPAD* is a dimeric enzyme, with each dimer containing 161 amino acids (figure 3).

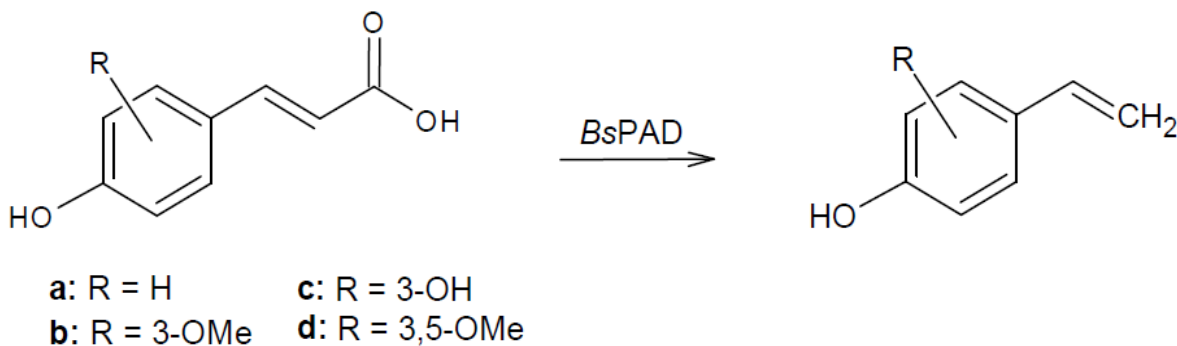


Figure 2. *p*-Hydroxycinnamic acid derivatives are converted to their corresponding *p*-hydroxystyrenes in reactions catalyzed by phenolic acid decarboxylase from *Bacillus subtilis* (*BsPAD*)

Size exclusion chromatography and X-ray crystallography showed that *BsPAD* is a homodimer with a molecular mass of 40 (2 x 20) kDa (Protein Data Bank code: 2P8G; Cavin et al., 1998). In each subunit, an internal cavity formed by a conserved β -barrel contains an active site which changes its conformation from ‘open’ to ‘closed’ via the movement of several loops upon substrate binding. An arginine residue (Arg41) forms a hydrogen bond with the phenol functional group, while two tyrosine residues (Tyr11 and Tyr13) engage with the carboxylate groups of the substrate. Glutamate (Glu64) is the catalytic base that accepts a proton from *p*-hydroxyl group (Frank et al., 2012).



Figure 3. 3D structure of phenolic acid decarboxylase from *Bacillus subtilis* (*BsPAD*) (generated by PyMOL 2.4). Red amino acid residues represent residues that are part of an active site

While PAD-type enzymes can decarboxylate several phenolic acids, substrate analogues that lack a hydroxy group at the *para*- position of the aromatic ring are converted much slower. Also, since neither sinapic acid nor 5-hydroxy ferulic acid could be decarboxylated by the enzyme, it was suggested that the substitution of both *meta*- sites on the aromatic ring prevents the biotransformation (Edlin et al., 1998). Morley and co-workers (2013) used the crystal structure of *BsPAD* to alter the substrate specificity by site-saturation mutagenesis. Based on the assumption that the active site of the *BsPAD* cannot accommodate hydroxycinnamic acids with bulky substitutions, such as sinapic acid, five amino acid residues of the *BsPAD* active site were targeted by saturation mutagenesis. Following a screening based on the absorbance of sinapic acid, a variant in which isoleucine at position 85 was substituted by alanine showed enhanced activity towards sinapic acid (Morley et al., 2013).

2.4. COMMONLY USED METHODS FOR DETERMINATION OF THE *p*-HYDROXYCINNAMIC ACIDS AND *p*-HYDROXYSTYRENE DERIVATES

Determination of the *p*-hydroxycinnamic acids and *p*-hydroxystyrene derivatives largely relies on complex and time-consuming methods.

2.4.1. Thin-Layer Chromatography (TLC)

The term chromatography implies the separation of complex mixtures into individual compounds between mobile and stationary phases (Belanger et al., 1997) that do not mix. The separation of individual compounds is based on the fact that the compound (analyte) from the solution interacts with stationary and mobile phase due to differences in adsorption, distribution between phases or the size of the substance being separated, which affects its retention time. It is the most basic way to confirm whether phenolic compounds are present in the mixture (Dinakaran, 2018). Despite its many advantages, TLC is a qualitative analytic method with limited quantitation capabilities. Because of this, TLC may be used to detect activity or assess the completion of a bioconversion, but it is not accurate enough to provide accurate quantitative data for the decarboxylation of *p*-hydroxycinnamic acids.

2.4.2. Gas Chromatography (GC)

Gas chromatography (GC) employs a solid stationary phase while the mobile phase is gaseous. Sample molecules are transported by the carrier gas through the GC system, ideally without any interaction. The speed of analyte passage through the column is determined by the ratio of its distribution between the gaseous mobile phase and the immobilized stationary phase. It is a highly efficient method for separating, identifying, and quantifying various phenolic species, including *p*-hydroxycinnamic acids. The main limitation of GC analysis is that phenolics have low volatility and must be derivatized (Capriotti et al. 2014).

A carrier gas system, injector, gas chromatographic column, detector, and data processing unit are all standard components of GC equipment. The nature of carrier gas can affect the

separation characteristics of the GC system as well as its detection sensitivity; therefore, it is typically a permanent gas with minimal or no adsorption capacity, such as hydrogen, helium, or nitrogen. When determining volatile phenolic compounds, the carrier gas most often used is helium (Payer et al., 2017; Zhou et al., 2015; Cabrita et al., 2012; Zuo et al., 2002) or nitrogen (Hu et al., 2015). Injectors deliver the sample to the column and are divided into two groups. On-column injectors deposit samples directly into the column, while vaporization injectors use high temperatures to vaporize samples quickly, mix them with a carrier gas and transport them to the column (Forgacs and Cserhati, 2003). The volatile phenolic compounds of the injected sample are separated in the GC column divided into packed and capillary columns of various dimensions. A packed column is a rigid metal or glass column filled with a thin layer of a high molecular weight polymer, while a capillary column is a very small internal diameter glass or fused-silica tube. Capillary columns have a higher separation capacity than packed columns, making them more frequently used in GC. The stationary liquid phase of GC columns has low vapor pressure, high chemical stability, relatively low viscosity at analysis temperature, selectivity for the sample components and good wetting capacity (Forgacs and Cserhati, 2003). Often used stationary phases for separating and identifying phenolic are capillary compounds either with polyethylene glycol stationary phase (Zhou et al., 2015; Cabrita et al., 2012) or with a mixture of 5 % phenyl and 95 % dimethylpolysiloxane (Payer et al., 2017; Hu et al., 2015). Many different detectors have been developed for the sensitive and selective detection and quantification of sample components (flame-ionisation, FID; nitrogen-phosphorus, NPD; flame photometric, FPD; thermal conductivity, TCD; chemiluminescence, *etc.*), but in recent decades, GC methods combined with various mass spectrometric (MS) detection system have found increasing application in GC analysis of phenolic compounds (Payer et al., 2017; Zhou et al., 2015; Hu et al., 2015; Zuo et al., 2002).

2.4.3. High-Performance Liquid Chromatography (HPLC)

High-Performance Liquid Chromatography (HPLC) is a frequently used separation method that uses small particles as column packing materials, so the stationary phase and the components following past it has a large surface area, improving separation for more precise determination. It

is the most commonly used separation technique to analyse phenolic compounds. Although conventional LC methods have yielded promising results in the past, the high complexity of phenolics has put sustained pressure on improved chromatographic performance to meet increasing analytical demands regarding resolving power, selectivity, and sensitivity (Kalili and Villiers, 2011). HPLC, which enables quantitative analysis of multiple phenolics in a significantly shorter time, quickly replaced traditional approaches in the 1980s. Since then, it has become the most often employed technique for identifying and analysing these compounds (Cheynier et al., 2012).

HPLC is divided into two major groups - (1) normal-phase HPLC, in which the stationary phase is hydrophilic, and the mobile phase is hydrophobic, and (2) reversed-phase HPLC, where the stationary phase is hydrophobic, and the mobile phase is hydrophilic. In reversed-phase HPLC, analysed compounds are eluted by decreasing polarity in the presence of an organic solvent, making them far more common for analysis of phenolic compounds (Suleymanova et al., 2019; Noda et al., 2015; Jung et al., 2013). HPLC columns are mostly packed with silica gel with a silanol group on the surface that provides a high adsorptive capacity and is used for chemical bonding. Frequently used bonded phases include C18, C8, and phenyl, which are chains attached to the surface of the silica gel. C18 is octyldecylsilan, which contains 18 carbons bound to the silica allowing for a larger surface area and longer interaction time between the bonded phase and the elutes. For identification and separation of *p*-hydroxycinnamic acids and their corresponding decarboxylated products, variations of C18 columns are used (Li et al., 2021; Williamson et al., 2020; Mittmann et al., 2019; Hu et al., 2015; He et al., 2011). Compounds eluted from the chromatographic column are detected based on their physicochemical properties. The following are frequently used for detection: light refraction, fluorescence, nuclear magnetic resonances, absorption in the UV-, VIS- and near-IR range and MS. In addition, the compounds can be derivatised in the pre-column or post-column process to obtain detectable properties. Even though many types of detectors are used in chromatography, diode array detectors (DAD) that record UV-VIS absorption spectra are among the most frequently utilised detection systems in liquid chromatography (Kuppusamy et al., 2020; Mittmann et al., 2019; Suleymanova et al., 2019; Hu et al., 2015). By passing UV light through the eluting sample mixture compounds, the analyte can be quantified by comparing the absorbance to calibration standards. The separation capabilities of LC

and the selectivity and sensitivity of the MS detector are combined in HPLC-MS (Pyrzynska et al., 2014), allowing the identification of individual phenolic compounds from the complex matrices (Fiorini et al., 2014; Torre-Carbot 2005). The apparatus consists of a mass spectrometer connected to high-performance liquid chromatography *via* an appropriate interface.

GC and HPLC-MS are preferred methods for separating and quantifying phenolic compounds (Mojzer et al., 2016). However, because both of these approaches are relatively expensive to buy and maintain, many laboratories decide to employ HPLC-UV detection, which is less expensive, comparable easy to use, and appropriate for routine analysis (Pyrzynska et al., 2014).

It is worth noting that one research group also used a UV-VIS spectrophotometric assay in order to screen mutants for sinapic acid decarboxylase activity after site-saturation mutagenesis. The decrease of sinapic acid absorbance was monitored at 310 nm. On the other hand, the overlap of UV absorption spectra of substrates and their corresponding decarboxylated products significantly complicates kinetic measurements, which is why there was an increasing need to optimize a quick and efficient assay for measuring PAD activity in real-time.

2.5. UV-VIS SPECTROSCOPY

Spectroscopy is a branch of physics that studies a physical system through observation effects related to the emission and absorption of electromagnetic radiation. Each form of spectroscopy uses a different part of the electromagnetic spectrum and thus includes a different type of excitation, in which the region of near-UV (190 to 400 nm) and VIS part of the spectrum (400-800 nm) causes the excitation of valence electrons and their transition to higher energy levels (figure 4). UV-VIS spectroscopy is used to analyse a wide range of compounds in the food and beverage industry, in clinical diagnostics, drug discovery, and environmental science (Franca and Nollet, 2017).

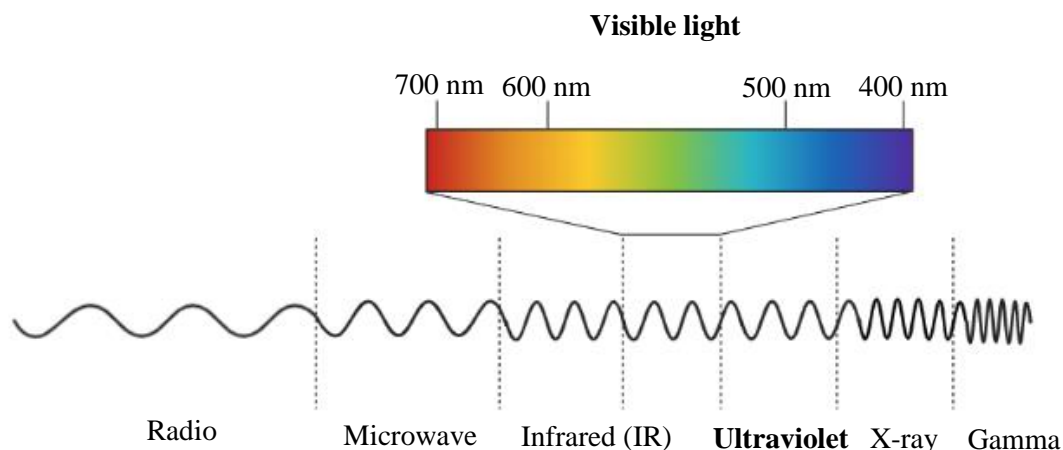


Figure 4. Electromagnetic spectrum

Photometric measurements are based on the absorption of light by conjugated double bonds. UV-VIS radiation corresponds to the energies that excite the molecule from its ground state or highest occupied molecular orbital (HOMO) to its excited state or lowest unoccupied molecular orbital (LUMO). The absorption energy in the UV range induces changes in the electronic energy of the molecule as a result of electron transitions. These transitions are related to electron excitation from bonding to antibonding orbitals. The energy of the photon and the electronic configuration of the molecule, that is, the energy differences between the electron states in the molecule, determine whether the molecule absorbs UV or VIS light. Because each molecule has a unique orbital structure, it will absorb light differently. This method relies on the measurement of the interaction of electromagnetic radiation with matter at a certain wavelength (Akash and Rehman, 2020). Depending on substitutions and the number of conjugated double bonds, phenolic molecules can absorb light across the UV-VIS range from 200-800 nm (Aleixandre-Tudo and du Toit, 2018; Harnly et al., 2007).

The spectrophotometer is used to analyze the absorption spectrum of electromagnetic radiation and measures the absorbance of the sample as a function of its wavelength. A light beam emitted from a suitable light source (UV or VIS) passes through the sample and is captured by a detector (Nilapwar et al., 2011). Typically, a light source emits polychromatic light (Akash and Rehman, 2020). Some of the radiation sources used are deuterium arc (190-330 nm) and tungsten

filament lamps (330-800 nm) that together generate a light beam that spans the UV-VIS spectral range. The intensity of a spectrophotometer light beam decreases when it passes through a UV-VIS active sample (figure 5). According to Beer-Lambert law [Eq. 1], there is a linear relationship between the concentration and the absorbance of the solution, where A is measured absorbance, ϵ molar absorption coefficient [$M^{-1}cm^{-1}$], c is solute concentration [M], ℓ is optical path length [cm], I_0 is incident light, and I is transmitted light.

$$A = \epsilon c \ell = \log (I_0/I) \quad [1]$$

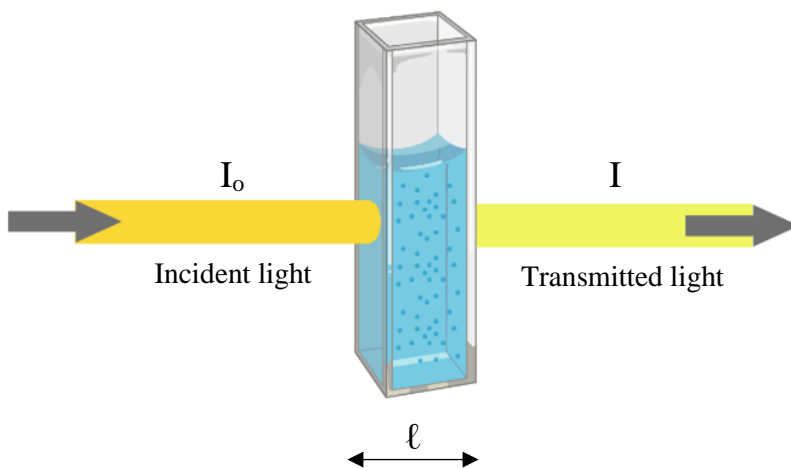


Figure 5. Working principle of Beer-Lambert law

In contrast to classic UV-VIS spectrophotometers, a plate reader is a similar appliance with few key differences. It significantly increases and accelerates throughput by using multiwell plates. Some plate readers can cover up to 1536 samples simultaneously. Because the conditions are consistent across the range of samples, the comparison of duplicates or triplicates is simplified. Typically, plate readers use a monochromator or filter-based optics. While the light beam in the spectrophotometer travels horizontally through the cuvette and the path length is standardized to 1 cm, light is passed vertically through the wells of a plate reader. The light beam orientation induces variables which must be considered, such as pipetting accuracy and consistency, since the volume within the well determines the path length.

3. EXPERIMENTAL PART

3.1. MATERIALS

3.1.1. Cell cultures

In this project, *Escherichia coli* BL21 (DE3) cells were used for the expression of BsPAD and variants thereof. Used *E. coli* BL21 (DE3) strains contained the pET28a plasmid with either the wild-type *pad* gene from *Bacillus subtilis* (accession number: WP_119995789) or its variant I85A. Both strains were obtained from the culture collection of the Institute of Molecular Biotechnology, Graz University of Technology.

3.1.2. Media used for the cultivation of *E. coli* BL21 (DE3) strain

- Lysogeny Broth (LB) medium (10.0 g/L peptone; 5.0 g/L yeast extract; 5.0 g/L NaCl)
- Terrific Broth (TB) medium (24.0 g/L yeast extract; 12.0 g/L tryptone, 4.0 g/L glycerol)
- 10X Terrific Broth (TB) salts (170 mM KH₂PO₄; 720 mM K₂HPO₄)

3.1.3. The column used for protein purification by affinity chromatography

- Ni Sepharose™ affinity column (GE Healthcare, USA)

3.1.4. Membrane used for imidazole removal

- Spectra/Por® 1 Dialysis Membrane (MWCO 6-8 kDa, Spectrum Labs, SAD)

3.1.5. Concentrator tube used for buffer exchange after protein purification

- Vivaspin® 20 centrifugal concentrator (10 kDa MWCO; Sartorius, Germany)

3.1.6. Kit used for protein quantification

- Bicinchoninic acid assay (Pierce™ BCA Protein Assay, ThermoFischer Scientific, USA) was used to determine the protein concentration of purified *BsPAD_wt* and *BsPAD_I85A* using bovine serum albumin as a calibration standard.

3.1.7. Well plates used in this research

- UV-STAR® well plates (96 Well UV-STAR® Microplate, Greiner Bio-One, Austria) used for spectrophotometric analysis
- Greiner microplate (Microplate, 96 well, PS, Greiner Bio–One, Austria) used for HPLC-UV analysis

3.1.8. Aluminium plates used for thin-layer chromatography (TLC)

- TLC Silica gel 60 F₂₅₄ (Aluminum sheets 20 x 20 cm; Merck KGaA, German)

Table 1. List of chemicals, buffers and standards used in this Graduate thesis

Chemical	Supplier
Acetic acid	Roth, Germany
Acetonitrile >99 % for HPLC	Chem-lab, Belgium
Bovine serum albumin standard	Sigma-Aldrich, USA
Caffeic acid (CAA)	Alfa Aesar by Thermo Fischer Scientific, USA
Coomassie Brilliant Blue G-250	Sigma-Aldrich, USA
<i>p</i> -Coumaric acid (<i>p</i> -CUA)	TCI Chemicals, USA
Deuterated chloroform (CDCl ₃)	Sigma-Aldrich, USA
Dimethyl sulfoxide (DMSO)	Sigma-Aldrich, USA
di-Potassium hydrogen phosphate (K ₂ HPO ₄)	Roth, Germany
Double distilled water (ddH ₂ O)	IMBT, TU Graz

Table 1. List of chemicals, buffers and standards used in this Graduate thesis – *continuation*

Ethanol (EtOH, 96 %)	Roth, Germany
Ferulic acid (FA)	Alfa Aesar by Thermo Fischer Scientific, USA
Glycerol	Roth, Germany
Hydrochloric acid (HCl)	Fischer Chemical, USA
Imidazole	Roth, Germany
Isopropyl- β -D-1-thiogalactopyranoside (IPTG)	Roth, Germany
Kanamycin	Roth, Germany
Methyl tert-butyl ether (MBTE)	Roth, Germany
Peptone	Roth, Germany
Potassium dihydrogen phosphate (KH ₂ PO ₄)	Roth, Germany
Sinapic acid	TCI Chemicals, USA
Sodium chloride (NaCl)	Roth, Germany
Sodium sulfate (Na ₂ SO ₄)	Roth, Germany
Terrific Broth (TB medium)	Roth, Germany
Tris aminomethane (TRIS)	Roth, Germany
Methyl tert-butyl ether (MBTE)	Roth, Germany

Table 2. Buffers, protein ladders and gels used in SDS-PAGE

Buffer/protein ladder/gel	Manufacturer
NuPAGE TM LDS Sample buffer (4X)	Thermo Fischer Scientific, USA
NuPAGE TM Reducing agent (2X)	Thermo Fischer Scientific, USA
NuPAGE TM MES Running buffer	Thermo Fischer Scientific, USA
PageRuler TM pre-stained protein ladder	Thermo Fischer Scientific, USA
NuPAGE TM 4-12% Bis-Tris gel	Thermo Fischer Scientific, USA

Table 3. Buffers used during purification and for activity and kinetic measurements of *BsPAD_wt* and *BsPAD_I85A*

Buffer	Composition
Potassium phosphate buffer (KPi)	50 mM potassium phosphate pH 6.0
Binding buffer	20 mM Tris-HCl 300 mM NaCl 30 mM imidazole pH 7.4

Table 4. Laboratory devices

Device	Model	Manufacturer
Analytical balance	Practum®	Sartorius, Germany
Centrifuges	5415 R	Eppendorf, Germany
	5810 R	Eppendorf, Germany
	Avanti® J-20 XP	Beckman coulter, USA
HPLC	Agilent 1200 Gradient HPLC System	Agilent Technologies, Austria
pH-electrode	inoLab® pH 720	VWR International, USA
Precision balance	CP 6201	Sartorius, Germany
Rotary Evaporator	Laborota 4011 digital	Heidolph, Germany
SDS-PAGE machine	PowerEase500 Invitrogen	Thermo Scientific, USA
Sonifer	Branson Ultrasonics™ Sonifier S-250A	Thermo Scientific, USA
Shaking incubator		Infors HT, Switzerland
Spectrophotometer	BioPhotometer 6131	Eppendorf, Germany
	NanoDrop™ 2000	Thermo Scientific, USA
	Plate reader	BioTek Instruments, USA
ThermoMixers®	ThermoMixer® comfort	Eppendorf, Germany
Vortex	Vortex-Genie 2	Scientific industries, USA

3.2. METHODS

3.2.1. Expression and purification of recombinant phenolic acid decarboxylases from *Bacillus subtilis* (*BsPAD_wt* and *BsPAD_I85A*)

3.2.1.1. Over-night cultures

Over-night cultures (ONCs) of chemically competent *E. coli* BL21 (DE3) cells transformed with the pET28a plasmid containing the wild-type *pad* gene or its variant I85A were prepared by supplementing 5 mL of Lysogeny broth (LB medium, see Chapter 3.1.2.) with the antibiotic kanamycin (final concentration: 40 mg/L). Kanamycin-supplemented LB media were inoculated with 10 µL of *E. coli* BL21 (DE3) glycerol stock (either with the *bspad_wt* containing strain or with the strain containing the *bspad_I85A* mutant). ONCs were incubated at 37 °C and 130 rpm for 16 h.

3.2.1.2. Heterologous expression of *BsPAD* wild type (*BsPAD_wt*) and *BsPAD* mutant (*BsPAD_I85A*)

After the inoculum preparation (see chapter above), *E. coli* BL21 (DE3) *BsPAD_wt* and *BsPAD_I85A* strains were grown at 400 mL-scale for protein expression and purification. For the main cultures, 400 mL of the TB medium was prepared. To this end, TB medium (see Chapter 3.1.2.) and 10X TB salts (see Chapter 3.1.2.) were prepared and autoclaved separately. After cooling down to room temperature, 90 % of TB medium was mixed with 10 % of 10X TB salts. Sterilized TB medium was added to a sterile 2 L baffled Erlenmeyer flask and supplemented with kanamycin to a final concentration of 40 mg/L. TB media were inoculated with 5 mL of the ONC [*E. coli* BL21 (DE3) *BsPAD_wt* or *BsPAD_I85A* strain]. The main cultures were incubated at 37 °C and 120 rpm with periodic determination of the optical density of the suspension at 600 nm (OD₆₀₀; BioPhotometer 6131, Eppendorf, Germany). After the OD₆₀₀ value reached 0.5-0.6 (usually ~3 hours after inoculation), gene expression was induced by adding isopropyl-β-D-1-thiogalactopyranoside (IPTG) to a final concentration of 0.1 mM. After induction, the bacterial cultures were cultivated at 24 °C and 130 rpm for about 24 h. Cells were harvested by centrifugation (4000 rpm, 4 °C, 15 min; Avanti J-10, Beckman coulter, USA), and the cell pellets were washed and resuspended in 20 mL of 50 mM potassium phosphate buffer (KPi), pH 6.0 (Table 3). After discarding the supernatant, cell pellets were either stored at -20 °C or used for protein purification. Prior to cell lysis, cell pellets were resuspended in the ‘binding buffer’ (Table 3).

3.2.2. Purification of expressed *BsPAD_wt* and *BsPAD_I85A*

Harvested cell pellets from the expression process (see chapter above) were thawed on ice and resuspended in 20 mL of 20 mM Tris-HCl ‘binding’ buffer (Table 3) to improve protein binding to the chromatography column during the purification process. Resuspended cell suspensions were sonicated at 4°C (output control: 50 %, duty cycle %, 5 min; Branson Ultrasonics™ Sonifier S-250A, Thermo Scientific, USA), and the cell debris were separated from soluble components by centrifugation (11 000 rpm, 4 °C, 30 min; Avanti J-25.50, Beckman coulter, USA). Obtained supernatants were filtered through a 0.22 μm Minisart® Syringe Filter (Sartorius,

Germany) to remove any residual macroscopic impurities. PADs were purified from the supernatants *via* Ni-affinity chromatography (GE Healthcare, USA). Approximately 1.5-2 mL of the Ni Sepharose™ resin (GE Healthcare, USA; see Chapter 3.1.2.) was placed in affinity gravity columns and washed with 5 column volumes (CV) of distilled water before use. After that, columns were equilibrated with 10 CV of binding buffer. Isolated proteins from each cell culture (*BsPAD_wt* and *BsPAD_I85*) were purified in an individual Ni Sepharose™ affinity column. The supernatant was applied to the column and incubated on ice for 30 min on a rotary shaker operating at 100 rpm. The flow through (FT) was collected and each column with bound enzymes was washed with 10-20 CV binding buffer to remove unspecifically bound proteins. All buffer-washed (BW) fractions were collected. Enzymes were eluted with 5-7 CV of elution buffer that contained 300 mM of imidazole, and collected in fractions of 1 mL. Columns were washed with 10 CV of elution buffer, rinsed with 10 CV of ddH₂O and 10 CV of 20 % ethanol (EtOH). Columns were filled with 20 % ethanol, sealed and stored at 4 °C.

Purified enzyme fractions were pooled and desalted to remove imidazole. Enzyme samples of approximately 5 mL were transferred to a Spectra/Por® 1 dialysis membrane (MWCO 6-8 kDa, Spectrum Labs, SAD) and incubated in a beaker filled with 300 mL 50 mM KPi buffer, pH 6.0. The solutions were incubated overnight in a cold room (4 °C), placed on a magnetic stirrer and gently stirred (cca. 5 rpm). Afterwards, desalted samples were concentrated by centrifugation (4000 rpm, 4 °C, 10 min; 5810 R, Eppendorf, Germany) using Vivaspin® 20 centrifugal concentrators (10 kDa MWCO; Sartorius, Germany) to a final volume of 1.5 mL.

3.2.3. Determination of phenolic acid decarboxylase concentration

A NanoDrop™ 2000 spectrophotometer (Thermo Scientific, USA) was used to determine absorbance of purified PAD proteins at 280 nm and therefrom respective concentrations by using molar absorption coefficients. The protein solutions were appropriately diluted for SDS-PAGE. In addition, protein concentrations of pooled and desalted fractions were determined using the BCA protein assay [solutions and protocols were used according to the manufacturer's instructions (Pierce™ BCA Protein Assay, ThermoFischer Scientific, USA), see Chapter 3.1.5.]. The absorbance of the obtained samples was measured at 562 nm using UV-STAR® well plates (96

Well UV-STAR® Microplate, Greiner Bio-One, Austria) using a plate reader (BioTek Instruments, USA).

3.2.4. Sodium dodecyl-sulfate polyacrylamide gel electrophoresis (SDS-PAGE)

The soluble protein fractions of the cell free extracts (CFE), as well as the fractions obtained during the purification of expressed proteins (see Chapter 3.2.2.) were qualitatively analyzed using gradient SDS-PAGE. This relatively fast, simple and highly sensitive electrophoretic method is often used after protein purification to confirm their expression and estimate the molecular weight of purified proteins. Gradient gels have a layer of polyacrylamide that gradually increases from the top to the bottom of the gel, which allows greater resolution when separating a wide range of protein molecular weights.

Aliquots of protein samples containing 5.9 µg/mL of protein were prepared according to the manufacturer's instructions by adding reducing reagent (10X, 2 µL; NuPAGE®, ThermoFischer Scientific, USA) and LDS buffer (4X, 4 µL; NuPAGE®, ThermoFischer Scientific, USA) to the sample solutions. The resulting mixtures were heated for 3 minutes at 96 °C and then applied to the wells of an gradient SDS-PAGE gel (4-12% Bis-Tris gel; NuPAGE®, ThermoFischer Scientific, USA). SDS-PAGE was performed in MES-SDS buffer at 160-180 V for 35 minutes (20X, PowerEase500®, ThermoFischer Scientific, USA). After that, the proteins in this gel were visualized with Coomassie Brilliant Blue (Sigma-Aldrich, USA) for approximately 8 h and destained according to the manufacturer's instructions (Sigma-Aldrich, USA).

3.2.5. Reaction conditions for complete substrates conversion for the TLC and ¹H NMR analysis

To test the decarboxylase activity of the purified proteins, decarboxylation products obtained by incubating *BsPAD_wt* and *BsPAD_I85A* with *p*-coumaric- (*p*-CUA), caffeic- (CAA), ferulic- (FA) and sinapic acid (SA) were analysed by TLC and ¹H NMR (see Chapters 3.2.5.1. and 3.2.5.2.). Due to the insolubility of the substrates in aqueous solvents, 200 mM stock solutions of the substrates were prepared in dimethyl sulfoxide (DMSO), a solvent highly miscible with water and a wide range of other organic compounds. Reactions were carried out in 1.5 mL vials in final

reaction volume of 1 mL with 50 mM KPi buffer, pH 6.0, and 10 mM of a substrate (*p*-CUA, CAA, FA or SA). The reaction mix was incubated on a Thermomixer comfort shaker (Eppendorf, Germany) at 30°C for approximately 10 min and 600 rpm. Then, *BsPAD_wt* was added to a final concentration of 0.4 mg/mL to reaction mixtures containing *p*-CUA, CAA or FA. The same concentration of *BsPAD_I85A* was added to a reaction mixture containing SA. The reactions were incubated for 3 h. Samples were taken after 0 h, 1 h and 3 h from the addition of the enzyme were analyzed by TLC (see Chapter 3.2.5.1.) and ¹H NMR (see Chapter 3.2.5.2.) to assess substrate conversion. After TLC had confirmed that all biotransformation processes were run to completion, converted products 4-vinyl phenol (4-VP), vinyl catechol (4-VC), 4-vinyl guaiacol (4-VG) and vinyl syringol (4-VS) were further used for the ¹H NMR analysis, and to prepare calibration standards for HPLC-UV (see Chapter 3.2.6.1.) and UV-VIS (see Chapter 3.2.7.1.) measurements.

3.2.5.1. Thin-layer chromatography (TLC)

TLC uses a stationary phase supported by an inert backing to separate components of a mixture. For separating and detecting hydroxycinnamic acids and their respective decarboxylation products, aluminium plates plated with polar silica gel were used as stationary phase. On a TLC Silica gel 60 F₂₅₄ (Aluminum sheets 20 x 20 cm; Merck KGaA, German), three different samples were applied: 2 µL of 10 mM substrate (*p*-CUA, CAA, FA or SA) as a standard, 2 µL of 0.4 mg/mL *BsPAD_wt* or *BsPAD_I85A* (depending on the substrate that was decarboxylated) and 2 µL of reaction samples removed from the biotransformation at different time points. TLC was run in a glass TLC chamber with a mixture of cyclohexane:ethyl acetate (1:1) as the mobile phase with the addition of 150 µL of acetic acid. TLC plates were incubated for approximately 5 min and dried with a heating gun before visualisation of the samples under the UV lamp.

3.2.5.2. ¹H NMR spectroscopy

For more explicit confirmation, decarboxylation of the substrates (*p*-CUA, CAA, FA and SA) was analysed by proton nuclear magnetic resonance spectroscopy (¹H NMR). After substrate conversion for 1-3 h (see Chapter 3.2.5.), reaction products were subjected to double extraction to remove the aqueous sample buffer. Methyl *tert*-butyl ether (MTBE) was added to samples at a

ratio of 1:1, after which the mixture was vortexed and centrifuged (13 000 rpm, 4 °C, 10 min; 5415 R centrifuge, Eppendorf, Germany). The organic phase was carefully transferred into a new reaction tube. An approximately equal volume of the organic solvent MBTE was added to the aqueous phase, and the extraction procedure was repeated. The organic phases were collected in a reaction tube and supplemented with an excess of Na₂SO₄ to bind the remaining water in the sample. Na₂SO₄ was added to each sample until the solution remained turbid when shaken, indicating saturation. Afterwards, the samples were placed in a rotary evaporator to evaporate the organic solvent. After evaporation, the sample was transferred to an NMR tube and mixed with 760 µL deuterated chloroform (CDCl₃). The height of the liquid in the NMR tube was 5 cm. CDCl₃ is a commonly used solvent in proton NMR spectroscopy. It is an isotopologue of chloroform in which the hydrogen atom has been substituted with deuterium. Sample tubes were placed in the NMR for analysis. This procedure was performed for each substrate (*p*-CUA, CAA, FA and SA).

3.2.6. HPLC-UV analysis

Decarboxylation reactions by the PAD enzymes were also followed by HPLC-UV, which is a commonly used chromatographic method in the literature. Since previous measurements of *Bs*PAD with HPLC-UV were already carried out at the Institute for Molecular Biotechnology, an established and optimized method was available.

3.2.6.1. HPLC calibration curve

Decarboxylation reactions were followed by determining the residual substrate concentration in PAD-catalysed biotransformations. Calibration standards were prepared using commercially available hydroxycinnamic acids at the highest purity available (*p*-CUA and SA, TCI Chemicals, USA; FA and CAA, Alfa Aesar by Thermo Fischer Scientific, USA). All substrates were prepared in HPLC-grade dimethyl sulfoxide (DMSO) at a concentration of 200 mM. Calibration standards were diluted in 50 mM KPi buffer, pH 6.0, to match the conditions used in the biotransformation reactions. 200 µL of substrate samples were transferred to Greiner microplates (Microplate, 96 well, PS, Greiner Bio-One, Austria) and covered with optical

adhesive covers (GPLE Thermo Fischer Scientific, USA) to prevent evaporation. Prior to measurement, well plates were centrifuged (13 000 rpm, 4 °C, 10 min; Eppendorf, Germany). After centrifugation, 150 µL of each sample was transferred to HPLC vials. For the calibration curve for HPLC-UV analyses the following concentrations of the substrates were used: 1.0, 2.5, 3.0, 5.0, 7.0, and 10.0 mM. All calibration standards were measured in triplicates.

3.2.6.2. Reaction conditions for the HPLC activity measurements

Each biotransformation reaction was performed at least in triplicates. Reaction mixtures were prepared by diluting the hydroxycinnamic acid substrates in 50 mM KPi buffer, pH 6.0, to a final concentration of 2.5 mM. The reaction mixtures were temperate to 30 °C for 10 min on a thermomixer operated at 450 rpm. The reaction was started by the addition of *BsPAD_wt* (0.0005 µg/µL, final concentration) or *BsPAD_I85A* (0.01 µg/µL, final concentration) to give a total reaction volume of 1.0 mL. *BsPAD_wt* was used for the decarboxylation of *p*- CUA, CAA and FA, and the *BsPAD_I85A* mutant was used to convert SA. Enzymes were added using a multichannel pipette set to mix three times to guarantee proper mixing.

To achieve time-dependent progress curves, samples were withdrawn periodically and quenched with acetonitrile (ACN), which instantly inactivates the enzyme, thereby stopping the reaction. 150 µL of sample solution was mixed with 150 µL of ACN, which was pre-prepared in Greiner microplates (Microplate, 96 well, PS, Greiner Bio–One, Austria) for each time point. Reaction samples were analyzed after 0 min (immediately after the time of enzyme addition), 1 min, 5 min, 15 min and 60 min. After stopping the reactions, well plates were covered with an optical adhesive cover (GPLE, Thermo Fischer Scientific, USA), and the precipitated enzymes were removed by centrifugation with Centrifuge 5415 R (13 000 rpm, 4 °C, 10 min; Eppendorf, Germany). Removal of enzymes was necessary to prevent clogging of the HPLC system. After centrifugation, 150 µL of the enzyme-free reaction mixture was carefully pipetted into vials for the HPLC-UV analysis.

3.2.6.3. HPLC measurements

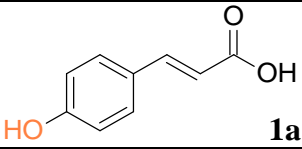
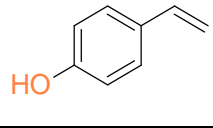
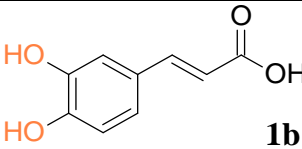
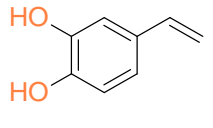
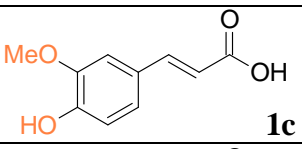
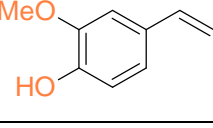
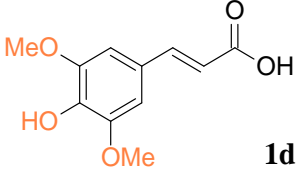
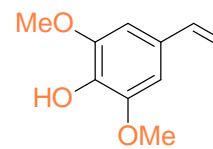
Samples were analyzed by Agilent 1200 Gradient HPLC System (Agilent Technologies, Austria) equipped with a diode array detector. In total, 2 μ L of each sample was injected into a reversed-phase Nucleodur C18 Pyramid column (5 μ m, 250 x 4.6 mm; Macherey Nagel, Germany). An isocratic HPLC method was used to separate the hydroxycinnamic acids. A combination of mobile phases was utilized for the elution at a total flow rate of 1 mL/min (Table 5). Previously purified by filtering, double distilled H₂O (ddH₂O) containing 0.1 % of acetic acid (solvent A), served as a water phase, and pure acetonitrile (ACN), which had already been used to quench the enzyme reactions, was used as the organic phase. The program of solvent A in B (v/v) used is described in detail in Table 5, and the retention times of substrates and their corresponding products are in Table 6. Elution was followed at 305 nm.

Table 5. Method parameters for the HPLC analysis of biotransformation products

Parameter	Method
Column	Reversed phase Nucleodur C18 Pyramid column (5 μ m, 250x4.6 mm; Macherey Nagel, Germany)
Injection volume	2 μ L
Mobile Phase	A: ACN B: ddH ₂ O (0.1 % acetic acid)
Flow	1 mL/min
Method	Isocratic
Program	0-13 min – 40 % ACN
Total program time	13.0 min

ACN-acetonitrile; ddH₂O-double distilled H₂O

Table 6. Retention time of substrates *p*-coumaric acid (1a), caffeic acid (1b), ferulic acid (1c) and sinapic acid (1d) and their decarboxylated products 4-vinyl phenol (2a), vinyl catechol (2b), 4-vinyl guaiacol (2c) and vinyl syringol (2d), detected at 305 nm with the HPLC-UV method

Substrate	Retention time (min)	Decarboxylation Product	Retention time (min)
 1a	3.2	 2a	2.8
 1b	3.9	 2b	3.2
 1c	4.1	 2c	3.3
 1d	3.9	 2d	3.2

3.2.7. Spectrophotometric assay for the determination of *Bs*PAD activity

Here we established a fast, robust and sensitive spectrophotometric assay for the activity measurements of PAD from *Bacillus subtilis* (*Bs*PAD_{wt}) and its I85A mutant (*Bs*PAD_{I85A}).

3.2.7.1. Measuring absorbance spectra and preparation of the calibration curve

Electronic absorbance spectra were obtained by measuring each sample at different wavelengths (250-500 nm). Calibration curves were necessary for the establishment of spectrophotometric assay. The substrate dilutions were prepared the same way described for HPLC-UV analysis (see Chapter 3.2.6.1.). The following concentrations of substrate solutions were prepared: 0.1, 0.2, 0.3, 0.4, 0.5, 0.6, 0.7, 0.8, 0.9, 1.0, 1.5, 2.0, 2.5, 3.0 mM in 50 mM KPi,

pH 6.0. 100 μL of dissolved substrate samples were pipetted in UV-STAR[®] microplate and the absorbance of the samples was measured spectrophotometrically with a BioTek Synergy HTX plate reader (Agilent Technologies, USA). The absorbance spectrum (250-500 nm) of each sample was measured. Product samples were obtained by complete *BsPAD_wt* decarboxylation of substrates (*p*-CUA, CAA, FA) and by *BsPAD_I85A* conversion of SA (see Chapter 3.2.5.). The same procedure was repeated for each enzymatically obtained decarboxylation product.

3.2.7.2. Reaction conditions for the *BsPAD_wt* and *BsPAD_I85A* activity measurements

Decarboxylation reactions were carried out in 1.5 mL reaction tubes in triplicates on a Thermomixer comfort shaker (Eppendorf, Germany) with continuous mixing at 450 rpm to maintain optimal reaction conditions. 2.5 mM of the substrate (*p*-CUA, CAA, FA and SA) was mixed with 50 mM KPi buffer, pH 6.0, and final reaction volumes were 1.0 mL. Reaction mixtures were tempered at 30 °C for 10 minutes. Reactions were started by adding a specific volume of enzyme solution using a multichannel pipette. The decarboxylation reactions of *p*-CUA, CAA and FA substrates are started by adding 0.0005 $\mu\text{g}/\mu\text{L}$ of *BsPAD_wt*. In comparison, the decarboxylation reaction of SA is carried out with the addition of 0.01 $\mu\text{g}/\mu\text{L}$ *BsPAD_I85A*. For measurement, 100 μL of the reaction mixtures were transferred to UV-transparent UV-STAR well plates (96 Well UV-STAR[®] Microplate, Greiner Bio-One, Austria) and continuously measured at the respective wavelength. The decrease in absorbance due to substrate consumption was monitored for 20 min.

3.2.7.3. Reaction conditions for the kinetics measurements

Kinetic measurements were conducted with the *BsPAD_wt*. Reactions were carried out in 1 mL 50 mM KPi buffer, pH 6.0, with addition 0.0005 $\mu\text{g}/\mu\text{L}$ of enzyme and with different substrate concentrations: 0.25, 0.5, 1.0, 1.5, 2.5, 3.0, 4.0, 5.0, 7.0 mM. Reaction conditions and measurements were conducted as previously described (see Chapter 3.2.4.2.) and used wavelengths for kinetic characterization are shown in Table 8. Based on the obtained results, K_M and V_{max} values were estimated.

4. RESULTS AND DISCUSSION

Biocatalytic decarboxylation of bio-based hydroxycinnamic acids offers a sustainable route to produce a variety of *p*-hydroxystyrene derivatives with broad applications as antioxidants, epoxy-coatings, adhesives and other polymeric materials (Schweiger et al., 2019). A current limitation in the application and engineering of phenolic acid decarboxylases is the lack of a robust and high-throughput enzyme assay for monitoring the decarboxylation reactions. State-of-the-art activity assays require extensive work-up, including product extraction and long analysis times. They are also limited to end-point measurements and lack real-time kinetic information. In this graduate thesis, a real-time and high-throughput setup for measuring real-time kinetics in the 96-well plate format was developed. The assay was tested for the conversion of the hydroxycinnamic acids: *p*-coumaric (*p*-CUA), caffeic (CAA), ferulic (FA) and sinapic acid (SA) employing phenolic acid decarboxylase from *Bacillus subtilis* wild-type (*BsPAD_wt*) or its I85A mutant (*BsPAD_I85A*).

Expression (Chapter 3.2.1.) and purification (Chapter 3.2.2.) of recombinant phenolic acid decarboxylases (*BsPAD_wt* and *BsPAD_I85A*) were conducted, and the purity of the enzymes was checked by SDS-PAGE (Chapter 3.2.4.). The complete conversion of substrates to their corresponding products was confirmed by TLC (3.2.5.1.) and ¹H NMR analysis (3.2.5.2.). The specific activity of *BsPAD_wt* and *BsPAD_I85A* was determined with HPLC-UV (Chapter 3.2.6.), which is a widely employed reference method to estimate concentration of substrates. It was used to test the accuracy of a newly established spectrophotometric assay for monitoring *BsPAD_wt* and *BsPAD_I85A* decarboxylation reactions. UV-VIS spectroscopy was used to acquire absorbance spectra and make calibration curves (Chapter 3.2.7.1.) for each substrate (*p*-CUA, CAA, FA and SA) and enzymatically obtained products (4-vinyl phenol, vinyl catechol, 4-vinyl guaiacol and vinyl syringol) in the 96-well plate format. Based on the individual molar absorption coefficients (Chapter 3.2.8.2.), the spectrophotometric assay was then used to measure Michaelis-Menten kinetics (Chapter 3.2.8.3.).

4.1. EXPRESSION AND PURIFICATION OF RECOMBINANT PHENOLIC ACID DECARBOXYLASE FROM *Bacillus subtilis* (*BsPAD_wt* and *BsPAD_I85A*)

4.1.1. Protein expression of *BsPAD* wild type (*BsPAD_wt*) and *BsPAD* mutant (*BsPAD_I85A*)

E. coli BL21 (DE3) cells transformed with expression vectors carrying genes coding for wild-type *BsPAD* or the I85A variant (Chapter 3.2.1) were used for heterologous expression of the *BsPAD_wt* and *BsPAD_I85A*. Expression of both target proteins could be observed by the separation of intense bands at 25 kDa in a SDS-PAGE gel (figure 6), which is in agreement with the molecular weight of a *BsPAD* monomer (Morley et al., 2013, Cavin et al., 1998) which is 20.02 kDa based on full amino acid sequence (Anonymous 2, 2007). Both proteins were obtained at high yield and high purity after a single-step chromatographic purification by the affinity chromatography.

The total yield of *BsPAD_wt* and *BsPAD_I85A*, as determined with the BCA protein assay, was 41.3 and 36.5 mg per liter of cultivation medium, respectively. Following purification, both proteins showed only minor impurities in SDS-PAGE (see Chapter 3.2.4., figure 6).

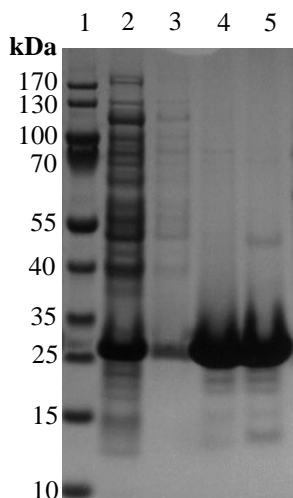


Figure 6. SDS-PAGE of purified *BsPAD_wt* and *BsPAD_I85A*. Lane 1: prestained protein ladder PageRuler™ (Thermo Fischer Scientific, USA); lane 2: cell free extract (CFE) of *BsPAD_wt*; lane 3: flow through (FT) of *BsPAD_wt*; lane 4: purified *BsPAD_wt*; lane 5: purified *BsPAD_I85A*

4.2. DETERMINATION OF *BsPAD_wt* AND *BsPAD_I85A* ACTIVITY BY THIN LAYER CHROMATOGRAPHY AND ¹H NMR

To overcome the low solubility of *p*-hydroxycinnamic acids in aqueous solutions, substrate stocks with a 200 mM concentration were prepared in the organic solvent dimethyl sulfoxide (DMSO). Low DMSO concentrations below 5% are tolerated by *BsPAD* enzymes (Schweiger et al., 2019). However, the highest substrate concentration achievable under these conditions was 10 mM.

4.2.1. TLC confirmation of substrates conversion

TLC was used as a qualitative method to confirm that the purified *BsPAD* enzymes (*BsPAD_wt* and *BsPAD_I85A*) possess decarboxylation activity and that complete conversion of the substrates (*p*-CUA, CAA, FA by *BsPAD_wt*, and SA by *BsPAD_I85A*) was achieved in biotransformation reactions. The time-dependent conversion followed by TLC analysis showed that FA was converted by *BsPAD_wt* within one hour, while all other substrates (*p*-CUA and CAA by *BsPAD_wt*, and SA by *BsPAD_I85A*) were converted within three hours.

In the figure 7a it can be clearly seen that one hour after adding the enzymes (*BsPAD_wt* when converting *p*-CUA, CAA and FA, and *BsPAD_I85A* in case of SA decarboxylation) to the reaction mixtures, in most cases, is short period of time for the full decarboxylation of phenolic acids. Although product formation can be easily observed, residual substrates that have not yet been decarboxylated are still visible near the baseline on the TLC plate. Three hours after starting the reaction, a complete substrates conversion to the desired products was observed (figure 7b, 7c, 7d and 7e).

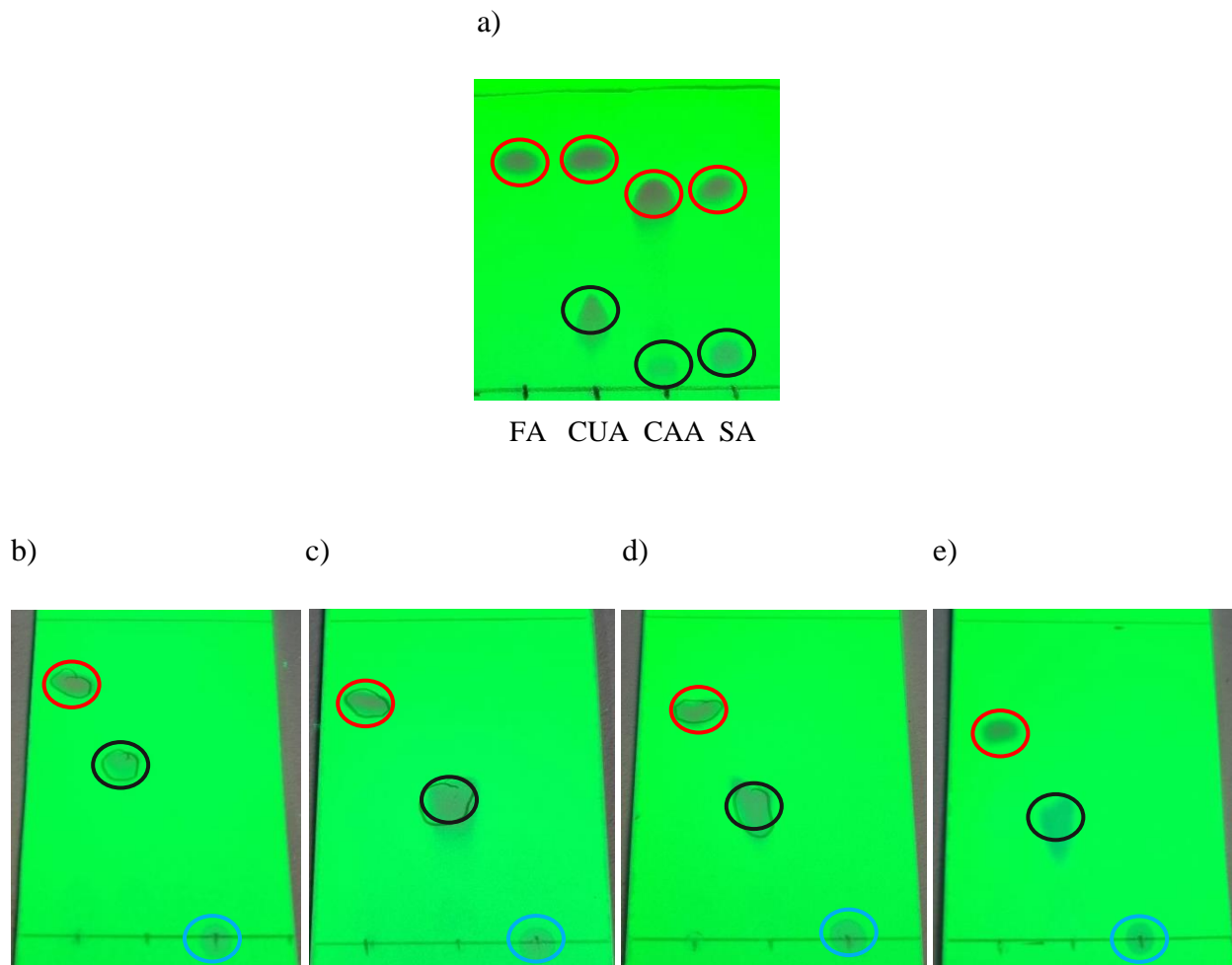


Figure 7. a) TLC of reaction mixtures (Rm) one hour after starting the decarboxylation reactions of *p*-CUA, CAA and FA (2.5 mM each) catalyzed by *BsPAD*_{wt} (0.005 μ g/mL) and SA (2.5 mM) catalyzed by *BsPAD*_{I85A} (0.01 μ g/mL). TLC of Rm three hours after starting decarboxylation reaction of: (b) *p*-CUA, (c) CAA and (d) FA by *BsPAD*_{wt}. TLC of Rm three hours after starting decarboxylation reaction of SA by *BsPAD*_{I85A}. Spots highlighted with red circles represent decarboxylated products 4-VP, 4-VC, 4-VG and 4-VS. Black circles represent 10 mM substrate standards (*p*-CUA, CAA, FA and SA), and blue circles represent *BsPAD*_{wt} or *BsPAD*_{I85A} enzyme dilution, also serving as standards

4.2.2. ^1H NMR confirmation of substrate conversion

Decarboxylation products obtained after full conversion of substrates (4-VP, 4-VG and 4-VS) were analysed by ^1H NMR spectroscopy and compared to commercially available *p*-hydroxystyrenes. After extraction of the reaction products with methyl tert-butyl ether (MTBE), samples were dissolved in a precisely determined volume of deuterated chloroform (CDCl_3 ; Chapter 3.2.5.2.).

An NMR spectrum of 4-VP obtained from *p*-CUA is shown in figure 8. Three olefinic protons (open-chain unsaturated hydrocarbons with at least one double bond) δ 5.1 (d, 1 H), δ 5.6 (d, 1 H), δ 6.6 (m, 1 H) and four aromatic protons (protons directly attached to a benzene ring) δ 6.7 (dd, 2 H), δ 7.3 (dd, 2 H) were observed, while one hydroxyl group could not be observed. The alcohol peak may not appear in the ^1H NMR because alcohols readily exchange hydroxyl protons. Exchange occurs between molecules with similar or different structures, and it is possible that the proton from the hydroxyl group exchanged with a deuterium atom from the chloroform (Xu et al., 2017). Additional peaks indicative of DMSO and water were also observed. The ^1H NMR spectrum of the enzymatically obtained 4-VP is in excellent agreement with the spectrum of the commercially available 4-VP standard (figure 9.). The spectrum of the used 4-VP standard contains an additional peak showing one hydroxyl group (R-O-H) δ 9.5 (s, 1 H) (figure 9.).

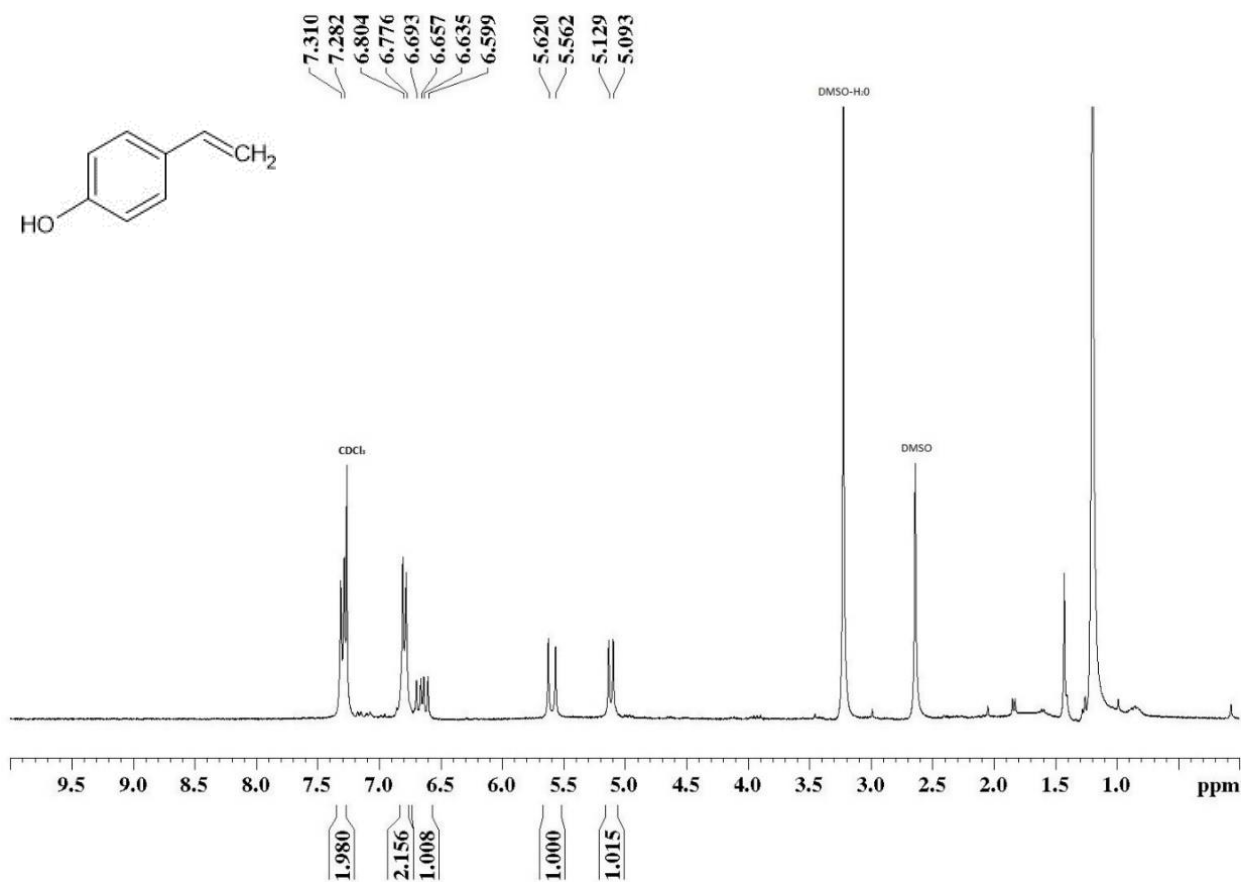


Figure 8. ¹H NMR spectrum of 4-VP obtained via *BsPAD_wt* decarboxylation of *p*-CUA

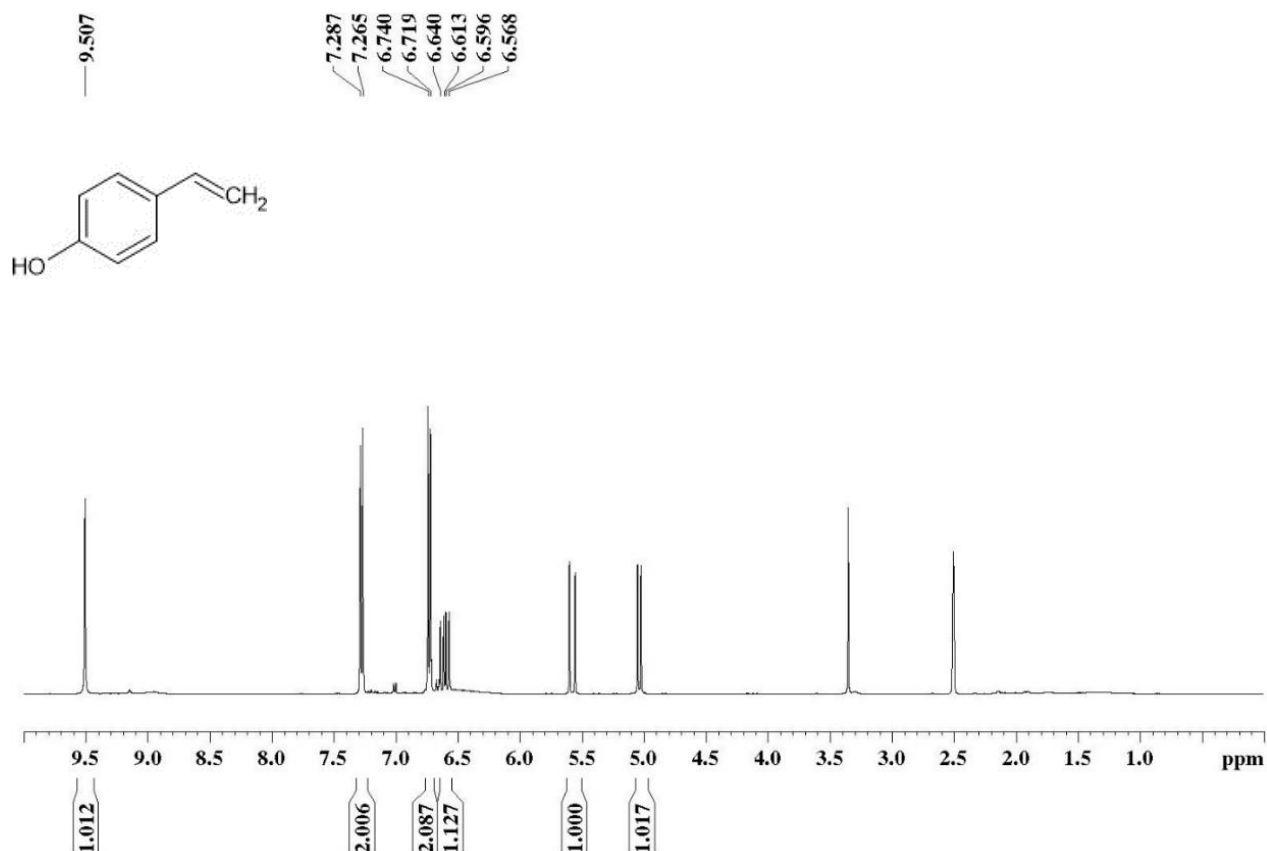


Figure 9. ^1H NMR analysis of the 4-VP standard

The ^1H NMR spectrum of 4-VG obtained from the enzymatic conversion of FA is shown in figure 10. It shows one methoxy group (R-O-CH_3) δ 3.9 (s, 3 H), one hydroxyl group (R-O-H) δ 5.75 (s, 1 H), three aromatic protons δ 6.85-6.95 (m, 3 H) and olefinic protons δ 5.1 (d, 1 H), δ 5.6 (d, 1 H), δ 6.6 (dd, 1 H). Again, additional peaks from the extraction of the resulting product were observed. Peaks indicative of H_2O δ 1.2, DMSO δ 3.2, MTBE δ 1.78 and δ 2.2 and the solvent CDCl_3 δ 7.26 were visible. However, the ^1H NMR spectrum of enzymatically obtained 4-VG is in agreement with the NMR spectrum of commercially available analytical grade chemical (Karmakar et al., 2000).

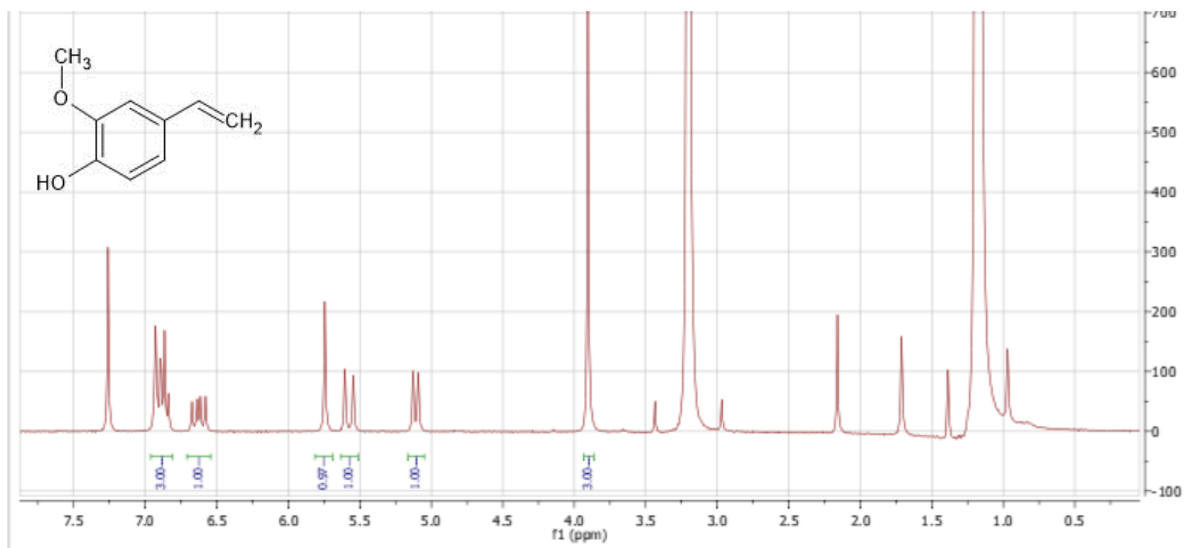


Figure 10. ¹H NMR spectrum of 4-VG obtained via *Bs*PAD_{wt} decarboxylation of FA

The ¹H NMR spectrum of enzymatically obtained 4-VS from SA is shown in figure 11. It showed two methoxy groups (R-O-CH₃) δ 3.90 (s, 6 H), three olefinic protons δ 5.1 (d, 1 H), δ 5.6 (dd, 2 H), two aromatic protons δ 6.60 (dd, 2 H), while one hydroxyl group was not observed. Results were comparable with chemically synthesized 2-methoxy-4-vinylphenol (4-VS) from the syringaldehyde (3,5-dimethoxy-4-hydroxybenzaldehyde) precursor (Zago et al., 2016). In alignment with the previous spectra, additional peaks indicative of water, DMSO, MTBE and CDCl₃ were observed.

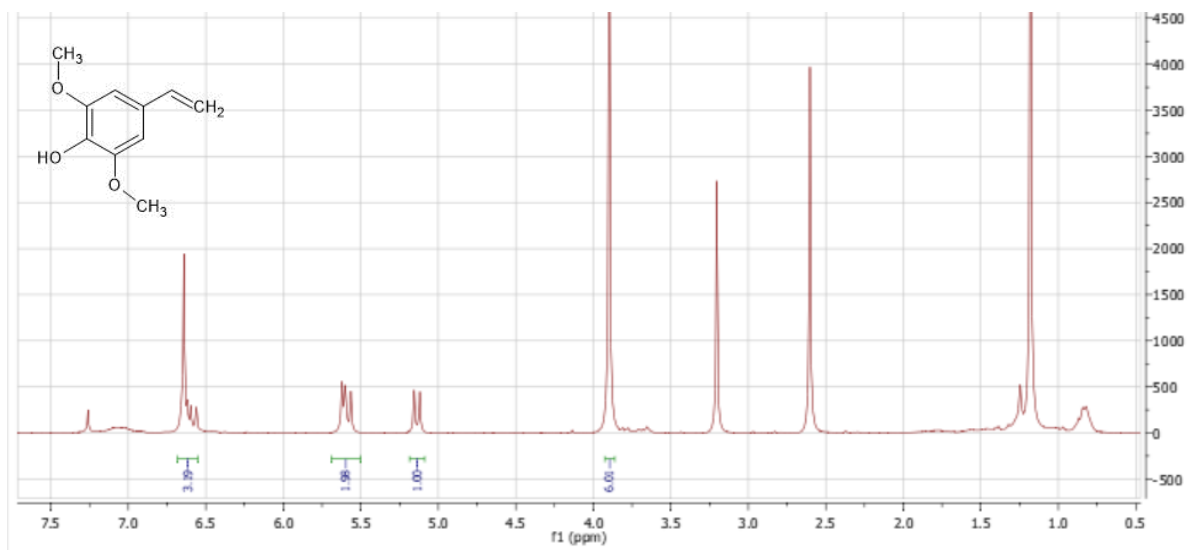


Figure 11. ¹H NMR spectrum of 4-VS obtained via *BsPAD_I85A* decarboxylation of SA

BsPAD_wt and *BsPAD_I85A* both generated NMR-pure *p*-hydroxystyrenes from the tested hydroxycinnamic acids (*p*-CUA, FA and SA). No traces of unconverted substrates could be identified. As a result, the protein-free products were used as calibration standards for HPLC-UV analysis and UV-VIS spectrophotometric assay.

4.3. DEVELOPMENT OF AN UV-VIS SPECTROPHOTOMETRIC ASSAY FOR THE ACTIVITY AND KINETIC MEASUREMENTS OF PHENOLIC ACID DECARBOXYLASE FROM *Bacillus subtilis*

4.3.1. UV-VIS absorbance spectra of substrates (*p*-CUA, CAA, FA and SA) and decarboxylated products (4-VP, 4-VC, 4-VG and 4-VS)

The herein described assay procedure builds on the well-known spectral features of substrates - *p*-hydroxycinnamic acids, which show absorption in the far- and near-UV range. Regarding the products, a simplified spectrophotometric method for detecting 4-VP initially reported by Cavin et al. (1993), which observed a hypsochromic shifts from 285-300 nm to 260 nm upon conversion of *p*-hydroxycinnamic acids to the respective decarboxylation products.

The first part of developing a fast, robust and sensitive spectrophotometric assay consisted of the accurate determination of molar absorption coefficients based on the absorbance spectra of each substrate (*p*-CUA, CAA, FA and SA) and the enzymatically converted products (see Chapter 3.2.7.1) at different wavelengths from 250 to 500 nm. UV-VIS spectra are created by recording the light intensity a sample absorbs, transmits or reflects depending on the wavelength. The main goal was to select wavelengths for each of the substrates and their respective decarboxylated products that do not overlap. Initially, electronic UV-VIS spectra of all *p*-hydroxycinnamic acids (*p*-CUA, CAA, FA and SA) and their corresponding *p*-hydroxystyrene products (4-VP, 4-VC, 4-VG and 4-VS) were recorded, and the corresponding molar absorption coefficients were determined (figure 12). All *p*-hydroxycinnamic acids showed similar spectral fingerprints with maxima at 290 to 320 nm.

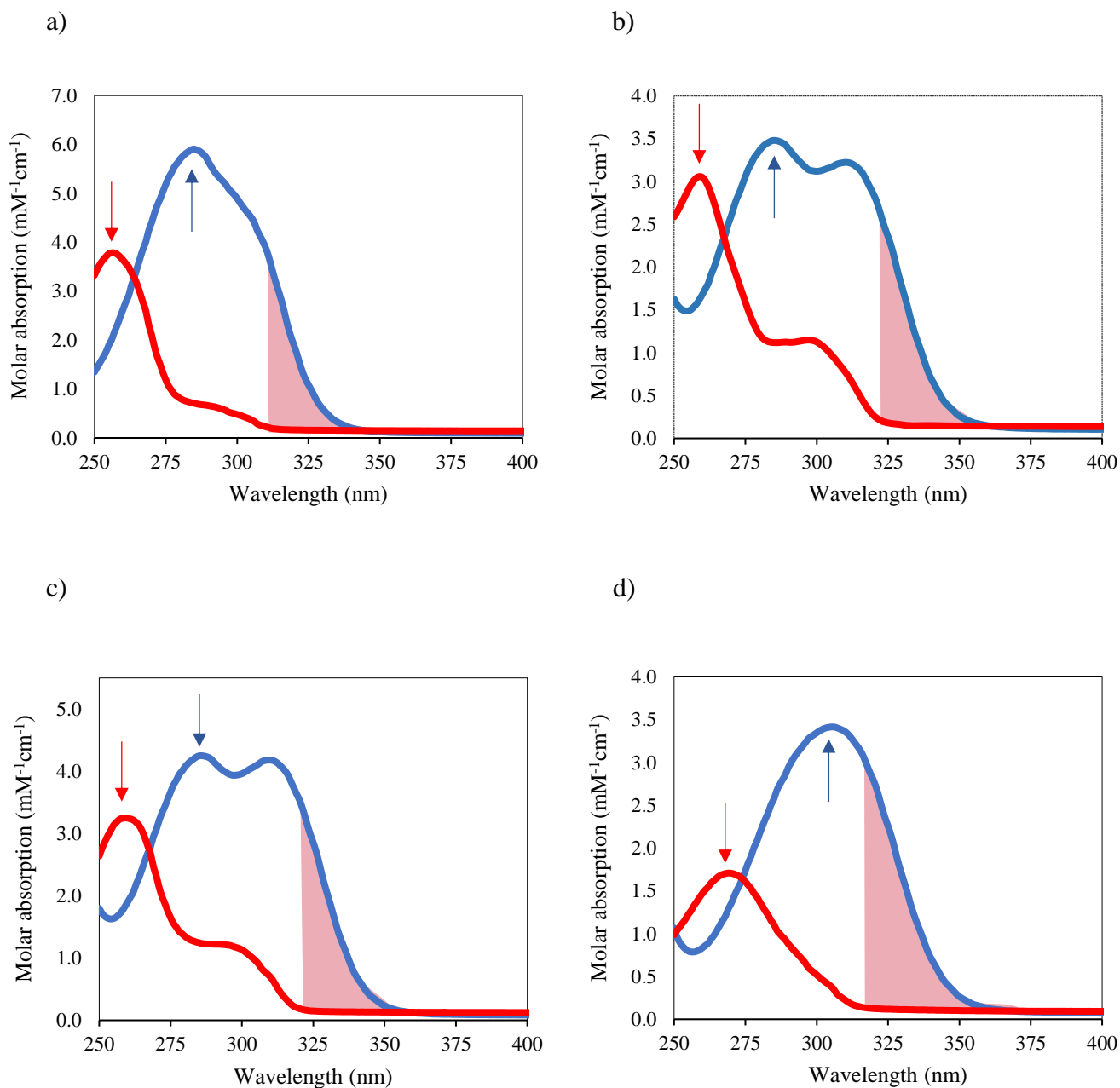


Figure 12. Molar absorption of 0.3 mM substrates *p*-CUA (a), CAA (b), FA (c) and SA (d) (blue line) and their corresponding decarboxylated 0.3 mM products 4-VP (a), 4-VC (b), 4-VG (c) and 4-VS (d) (red line) that were obtained after full enzymatic conversion of substrates. The shaded area below the blue line indicates the region where no overlap between the absorbance of the substrates and their decarboxylated products was observed. Blue arrows point to the maximum molar absorbance of each substrate, while red arrows point to the maximum molar absorbance of the products

The method described in this thesis finally enabled the determination of the time-dependent residual substrate concentration (substrate conversion) in a real-time assay. In the following, the assay procedure was optimized to accommodate high substrate concentrations ($> K_M$), while maintaining accurate measurement conditions.

The procedure was optimized for the 96-well plate format. Initially, absorbance spectra were recorded from 250-500 nm using commercially available substrate solutions (*p*-CUA, CAA, FA and SA) and enzymatically decarboxylated products (4-VP, 4-VC, 4-VG and 4-VS). Different concentrations of mentioned phenolic compounds were measured in a UV-VIS plate reader (see Chapter 3.2.8.1.). Figure 12. shows comparisons of the absorption spectra of commercially available substrate solutions and their converted products. Each absorption spectrum shows a different region of wavelengths (red shading) at which substrate and product absorption did not overlap. Thus, for each substrate, there is a different part of the spectrum in which the substrate's consumption can be measured without the influence of the product formation. During the substrate conversion, carboxyl group is removed, which changes the structure and conjugation of the obtained product, ultimately leading to a hypsochromic shift. In the example of *p*-CUA (figure 12.a) it can be seen that the maximal absorbance of the substrate is at 290 nm. In comparison, the maximum absorbance of the converted product, 4-VG, is at 260 nm. These findings agree with previously reported values for *p*-hydroxycinnamic acids (Miyagusuku-Cruzado et al., 2020). In the region between 310-330 nm, the substrate absorbs light, but the product does not, and based on that, a particular wavelength was chosen at which enzyme activity and kinetic measurements were carried out. In addition to the enzymatic decarboxylation of *p*-CUA, the mentioned hypsochromic shift appeared during CAA and FA (*Bs*PAD_wt) and SA (*Bs*PAD_I85A) conversion. For each substrate, a specific wavelength was selected for further analysis (table 7). These measurements were carried out in 96-well plates using a plater reader.

Table 7. Wavelengths selected for monitoring decarboxylation reactions of *p*-CUA, CAA and FA by *BsPAD_wt* and conversion of SA by *BsPAD_I85*

Enzyme	<i>BsPAD_wt</i>			<i>BsPAD_I85A</i>
Substrate	<i>p</i> -CUA	CAA	FA	SA
Wavelength (nm)	324	337	335	339
Molar absorption coefficient (M ⁻¹ cm ⁻¹)	3.57	3.63	3.78	3.63

Based on selected wavelengths, different substrate and product concentrations (0.1-3.0 mM) were prepared, and their absorbances were measured (see Chapter 3.2.7.1.). The measured UV-VIS absorption values showed a linear correlation with the concentration of the individual compounds. Based on this, calibration curves were created (figure 13) and used to calculate the molar absorption coefficients (table 7).

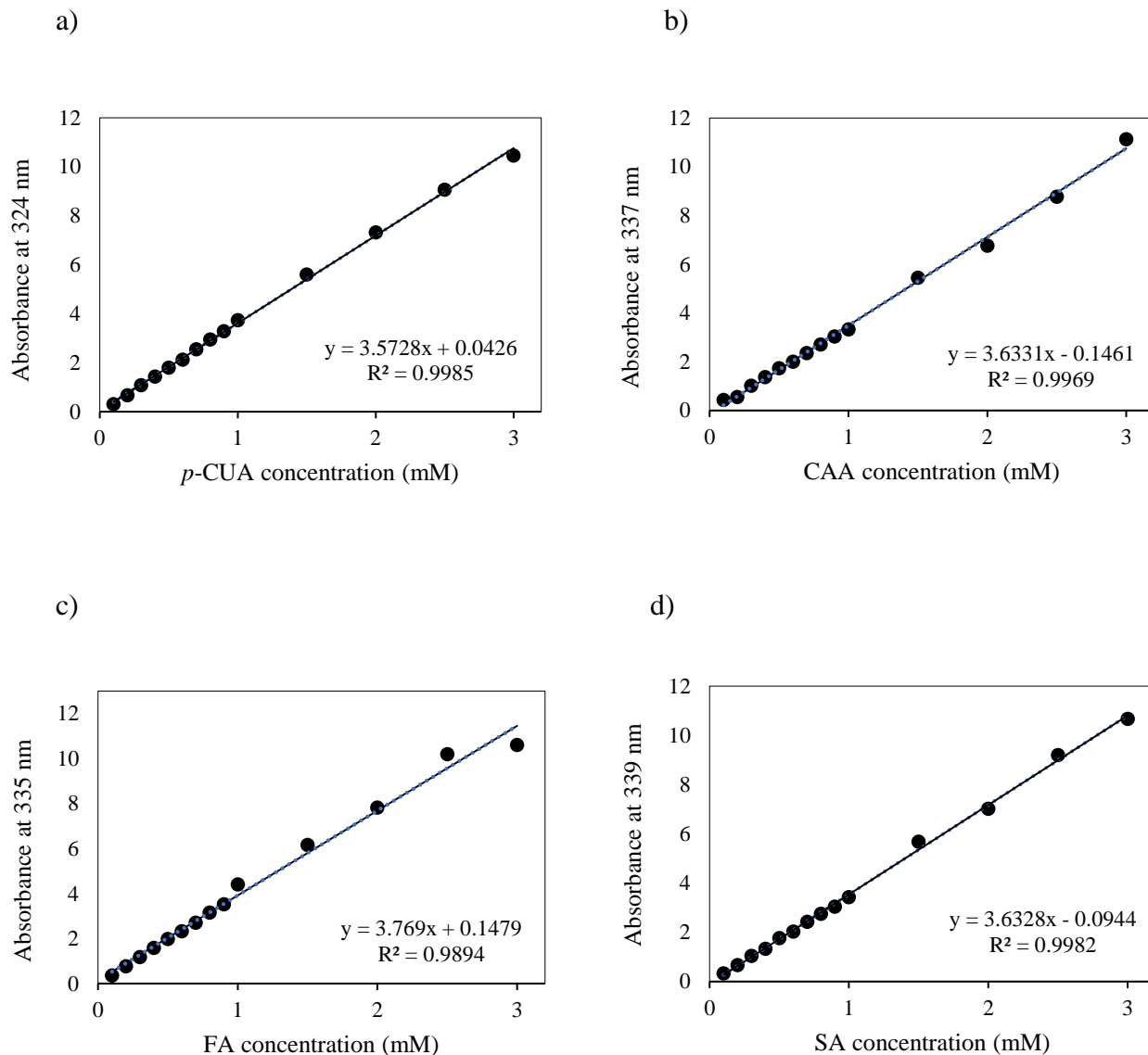


Figure 13. Calibration curves for *p*-CUA (a), CA (b), FA (c) and SA (d) at different wavelengths, used for further UV-VIS spectrophotometric phenolic acid decarboxylase (*BsPAD*_{wt} and *BsPAD*_{I85A}) activity measurements

Due to the high absorbance of the substrates (figure 13), substrate concentrations higher than ~1 mM saturated the detector and were not measurable with the standard 96 well-plate protocols. In order to expand the concentration range of the assay, different volumes of reaction mixture (50-100 μ L) in wells were tested. Considering pipetting errors and evaporation effects in

longer measurements, the most accurate results were obtained when using a total reaction volume of 100 μL in each well, while lower volumes did not yield reproducible results. In addition, the linearity of the molar absorption was tested at higher wavelengths from 324 nm (*p*-CUA), 337 nm (CAA), 335 nm (FA) and 339 nm (SA) up to 344 nm. With this, the substrate concentration in the reaction mixture could be increased to 7.0 mM. From there, 2.5 mM was the chosen concentration for further activity measurements.

4.3.2. Comparison of specific activity of *BsPAD_wt* and *BsPAD_I85A* followed by the HPLC and UV-VIS spectroscopy

The specific activity generated by UV-VIS spectroscopic assay for the wild-type and the I85A mutant were compared with the values obtained by HPLC, which is the most commonly used method to follow PAD activity (see Chapter 4.3.). The first part of establishing the HPLC-UV assay was to create calibration curves of each substrate and their decarboxylated product. Samples of various substrate concentrations (1.0-10.0 mM) were prepared, and their absorbance was measured with HPLC-UV (see Chapter 3.2.6.1.). All calibration samples were prepared in quadruplicates. Collected absorbance results were proportional to substrate concentration of each sample and based on that, resulting standard calibration curves were created (figure 14) and used for HPLC-UV *BsPAD_wt* and *BsPAD_I85A* activity measurements.

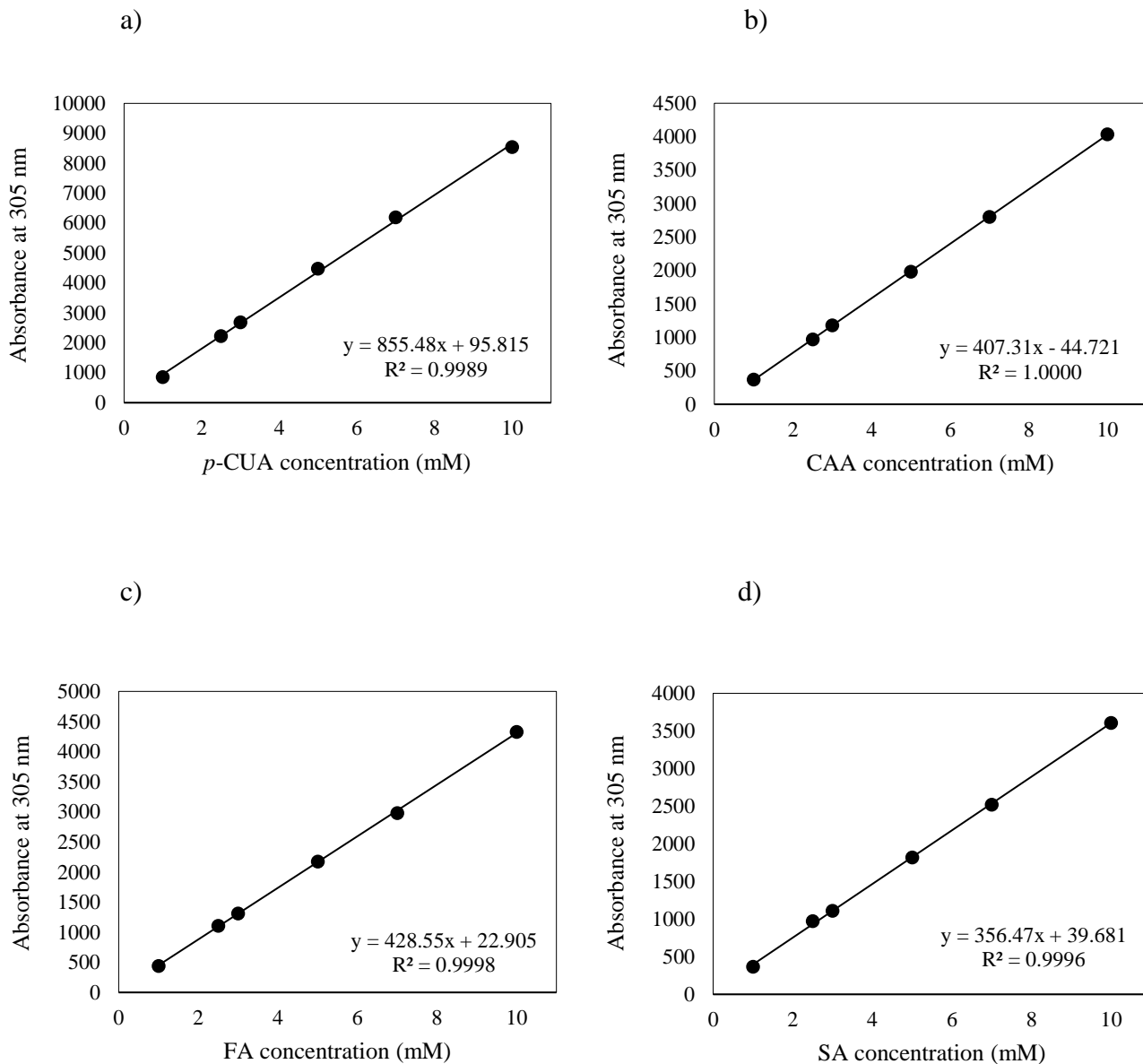


Figure 14. Calibration curves for *p*-CUA (a), CAA (b), FA (c) and SA (d) created by using the HPLC-UV method

An UV-VIS spectrophotometric assay development started by attempting to obtain maximally similar reaction conditions to compare the spectrophotometric assay with the HPLC-UV measurements. The specific activity of *BsPAD_wt* and *BsPAD_I85A* was determined using an established HPLC-UV method (see Chapter 3.2.6.3) using gradient HPLC System equipped

with a DAD detector (Agilent Technologies, Austria) and the obtained values were later compared with the results obtained using the UV-VIS spectrophotometric method. One of the goals was to quench the reaction at the same time points as when measured by HPLC-UV assay and then measure absorbance of the samples spectrophotometrically. One attempt of reaction quenching was using acetonitrile (ACN), which is commonly used to stop enzyme reactions (*e.g.* for HPLC-UV analysis). Other attempts to quench the reaction were by using hydrochloric acid (HCl) and freezing sample aliquots with liquid nitrogen. However, ACN led to a change in the absorption spectrum. When ACN was used, each HPLC-UV analysis was performed in triplicates or quadruplicates, and the results showed excessive errors in absorbance. Quenching the reactions using HCl also led to spectral changes, and repeats showed significant deviations in absorbance making this method unsuitable. Freezing the samples in liquid nitrogen caused only short-term inactivation of the enzyme. As a result of these quenching experiments, the reactions were followed in a photometer by starting reactions by adding *BsPAD_wt* or *BsPAD_I85A*, and absorbances were measured in a real-time for 60 min (see Chapter 3.2.8.2). The substrate concentrations in these experiments were set to 2.5 mM, which is within the measurement range of the UV-VIS photometric assay and HPLC-UV analysis.

Figure 15 compares the residual substrate concentration during *BsPAD*-catalyzed reactions quantified in time-dependent manner by the UV-VIS spectrophotometric assay and discontinuous analysis by HPLC-UV.

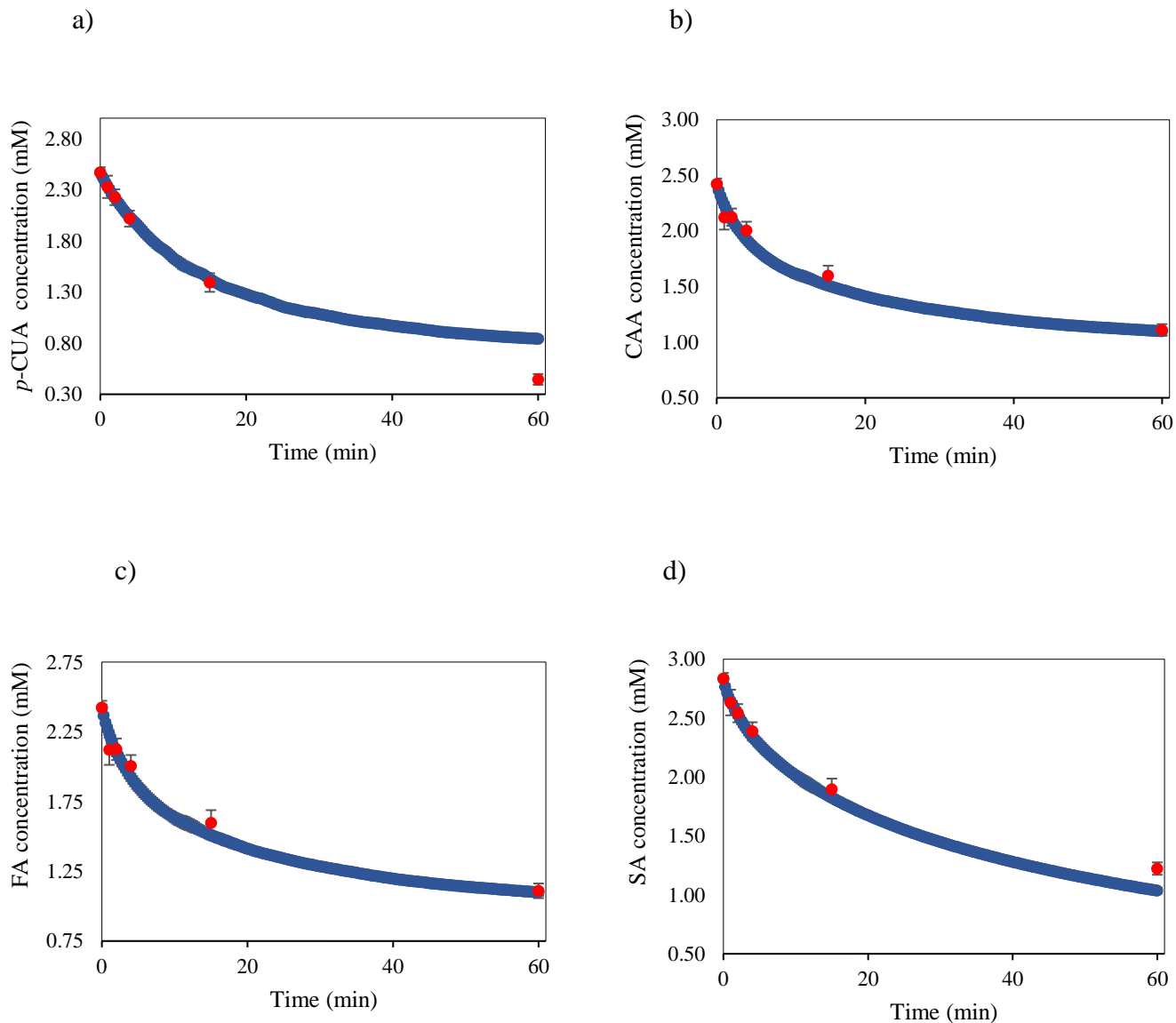


Figure 15. Comparison of substrate consumption by *BsPAD_wt* (*p*-CUA, CAA and FA) and *BsPAD_I85A* (SA) as determined by HPLC-UV analysis (red dots) and the UV-VIS photometric detection (blue curve)

Firstly, it can be noticed that measured absorbances by both methods show a strong overlap at the same time points. This fact supports the accuracy of the collected results by novel spectrophotometric assay. Also, important to mention is that the spectrophotometric assay generated significantly more data points when compared with the HPLC-UV analysis since the

previous one acquires the absorbance every 30 s. This way, substrate conversion is monitored in real-time from the beginning of the reaction. Because the *BsPAD* enzyme is stable and fast, the photometric measurements in the 96-well plate format allowed to simultaneously measure a large number of samples, with the results being obtained within 20 min. When the novel spectrophotometric assay is compared to the HPLC-UV method, the latter one requires several hours for similar number of samples.

Table 8 compares the specific activities of the wild-type and I85A *BsPAD* mutant obtained by the two analysis methods – HPLC-UV and the novel photometric assay. Both methods showed similar progress curves, as can be easily seen in the figure 15, the very accuracy of the spectrophotometric method is confirmed by the highly similar values of specific activities of the enzymes towards different substrates.

Table 8. Comparison of specific activities of *BsPAD*s determined by the HPLC-UV assay and by the spectrophotometric method in plate reader

Enzyme	<i>BsPAD_wt</i>						<i>BsPAD_I85A</i>	
	<i>p</i> -CUA		CAA		FA		SA	
Substrate	Specific activity (U/mg)	Std. error						
HPLC	243.50	86.93	144.0	88.07	297.90	52.81	14.60	0.85
Plate reader	243.90	59.41	143.0	18.54	315.40	8.33	14.40	1.68

Regarding all decarboxylation reactions, conventional natural *p*-hydroxycinnamic acids, such as *p*-CUA, CAA and FA, are readily accepted by wild-type *BsPAD* that in first few minutes after starting the reaction in the reaction mixture, shows very high specific activity. *BsPAD_wt* showed the highest specific activity towards converting FA, and the lowest towards CAA (table 8).

4.3.3. Determination of the kinetic constants (K_M and V_{max} values) of *BsPAD_wt* for *p*-CUA, CAA and FA

In the following, the spectrophotometric assay was used to estimate kinetic constants - K_M and V_{max} values for the decarboxylation of *p*-hydroxycinnamic acids (*p*-CUA, CAA and FA) by *BsPAD_wt* in 96-well plates. To this end, different substrate concentrations were used in reaction mixtures in range 0.25 - 6.0 mM and changes in absorbance of the reaction mixture were followed at different wavelengths for each substrate (table 9). Initial slopes of the reactions were used to calculate enzyme activities, which were fitted to the Michaelis-Menten equation for two substrates – *p*-CUA and FA, or to the Michaelis-Menten equation with substrate inhibition for CAA. Resulting Michaelis-Menten graphs are shown in figure 16 and estimated kinetic constants in table 10.

Table 9. Wavelengths used in the novel spectrophotometric assay for kinetic characterization of *BsPAD_wt*

Enzyme	<i>BsPAD_wt</i>		
Substrate	<i>p</i> -CUA	CAA	FA
Wavelength (nm)	329	344	344

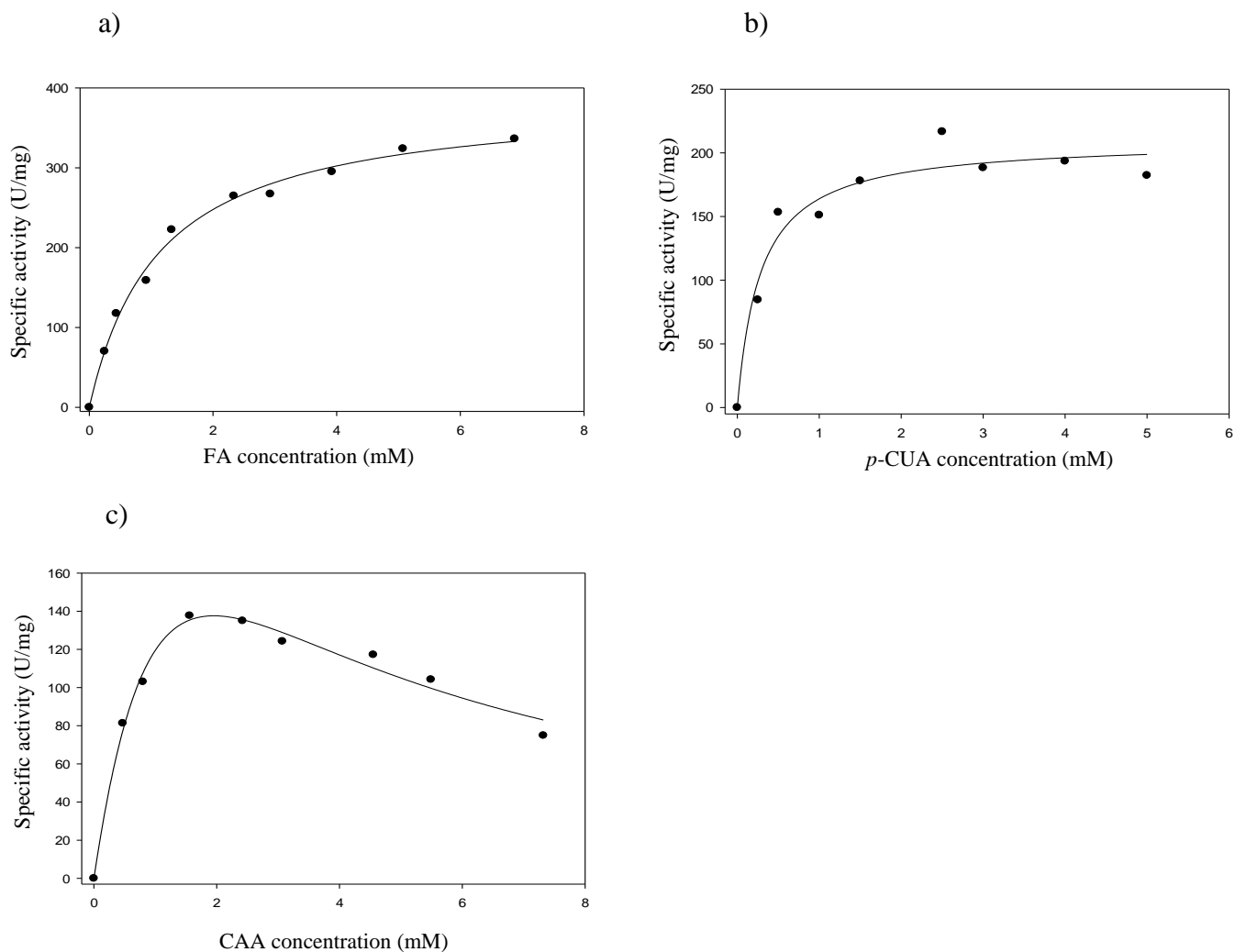


Figure 16. Michaelis-Menten curves generated for estimation of K_M and V_{max} for *BsPAD_wt* catalyzed decarboxylation of *p*-CAA (a), CAA (b) and FA (c)

Table 10. Determined kinetic constants of *BsPAD_wt* catalyzed reactions

Substrate	K_M (mM)	V_{max} (U/mg)	Std. error (V_{max}) (U/mg)
<i>p</i> -CAA	1.83	395.35	104.71
CAA	0.28	209.91	10.98
FA	1.34	403.59	12.21

For all three tested substrates, high V_{\max} values were obtained. Also their K_M values were different. The highest affinity was found for CAA (0.28 mM), while for *p*-CUA and FA had considerably higher K_M values were obtained - 1.83 and 1.34 mM, respectively. The obtained kinetic constants are in agreement with the values known from the literature (Cavin et al., 1998).

All assays were performed in UV-transparent 96-well plates using low volumes and low enzyme concentrations. The use of liquid handling equipment allowed simultaneous measurement of multiple samples, thus increasing the throughput. However, the reproducibility of the assays was high, indicated by low standard deviations (typically < 7%).

4.3.4. PAD activity assay protocol

Based on the obtained results, we propose the following assay protocol to measure PADs decarboxylation activity (figure 17):

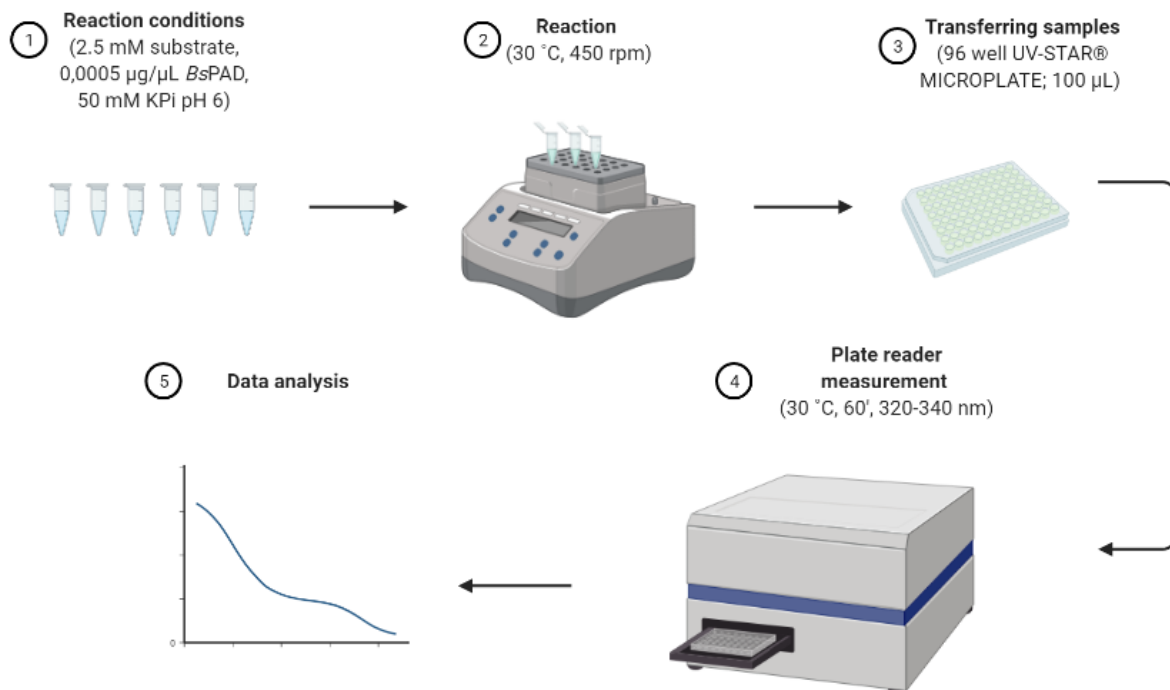


Figure 17. Proposed protocol for the novel spectrophotometric assay

Step 1: Prepare a 50 mM potassium-phosphate buffer (KPi; or another suitable buffer), pH 6.0. Prepare 10 mM substrate (*p*-CUA, CAA, FA or SA) stock solution in 50 mM KPi buffer, pH 6.0. Also prepare appropriate enzyme dilutions (*BsPAD*_wt in case of *p*-CUA, CAA, FA conversion or *BsPAD*_I85A in case of SA decarboxylation) in the 50 mM KPi buffer, pH 6.0.

Step 2: Reactions are carried out in 1.5 mL reaction tubes to the final reaction volume of 1.0 mL. Dilute substrate stock solution in reaction tubes with the 50 mM KPi buffer, pH 6.0, to final concentration of substrate of 2.5 mM and adjust temperature at 30 °C, 450 rpm for 10 min.

Reactions are started by the addition of enzyme solution (final *BsPAD*_wt concentration of 0.0005 $\mu\text{g}/\mu\text{L}$ or *BsPAD_I85A* concentration of 0.01 $\mu\text{g}/\mu\text{L}$) to the reaction tubes using a multichannel pipette. Pipette should be previously set to mix the reaction mixture after addition of enzyme 3 x.

Step 3: Immediately after mixing, with the same multichannel pipette, transfer 100 μL of each sample to the UV-transparent 96 well plates.

Step 4: Insert the well plate in the plate reader and start the absorbance measurements at 320-340 nm (depending on the measured substrate conversion) for 60 minutes.

5. CONCLUSIONS

Based on the results obtained within this Graduate Thesis, the following conclusions can be drawn:

1. *Bacillus subtilis* phenolic acid decarboxylase (*BsPAD_wt*) and its variant *BsPAD_I85A* were successfully expressed in *E. coli* BL21 (DE3) and purified by the affinity chromatography. Molecular weight of both monomers (*BsPAD_wt* and *BsPAD_I85A*) expressed with high yield (41.3 mg/L and 36.5 mg/L, respectively) was estimated by using SDS-PAGE to approximately 25 kDa.
2. Activity of the two variants (*BsPAD_wt* and *BsPAD_I85A*) towards *p*-hydroxycinnamic acids (*p*-coumaric acid, *p*-CUA; caffeic acid, CAA; and ferulic acid; FA for *BsPAD_wt*; and sinapic acid, SA for *BsPAD_I85A*) was qualitatively confirmed by using TLC and ¹H NMR.
3. Since current methods to kinetically characterise industrially relevant decarboxylation reactions of phenolic acids rely on HPLC, MS, GC or NMR methods, which require extensive sample work-up while measuring only endpoint concentrations, development of a fast, robust and sensitive spectrophotometric assay allowing following decarboxylation reactions in real-time while avoiding product extraction was in high demand. Therefore, absorbance spectra for each substrate (*p*-CUA, CAA, FA, and SA) and corresponding products (4-vinyl phenol, 4-VP; vinyl catechol, 4-VC; 4-vinyl guaiacol, 4-VG; and vinyl syringol, 4-VS) were acquired and range of wavelengths with no substrate/product overlap were defined. Further, calibration curves for the substrates (*p*-CUA, 324 nm; CAA, 337 nm; FA, 335 nm; and SA, 339 nm) were created and molar absorption coefficients for each substrate estimated.
4. Protocol for spectrophotometric assay was established and used for determination of *BsPAD_wt* and *BsPAD_I85A* activity. Obtained results expressed as specific activity are completely in agreement with data collected by the HPLC-UV method in common practice.
5. The established spectrophotometric assay was then used to estimate kinetic parameters (K_M and V_{max}) for three substrates (*p*-CUA, CAA, and FA) decarboxylated by *BsPAD_wt*. The enzyme showed higher affinity towards CAA (K_M of 0.28 mM) than for *p*-CUA and FA (K_M of 1.34 and 1.38 mM, respectively).

6. Using *Bs*PAD as a model PAD, the spectrophotometric assay procedure was optimized for use in microtiter plates, allowing fast and real-time measurement of enzyme activities. This procedure requires considerably lower enzyme amounts (0.5-10 μg), while no sample workup is needed. The availability of a fast and robust assay that is high-throughput ready allows, for example, to screen mutagenesis libraries for improved variants, or can help identifying new decarboxylases. Thus, the herein described enzyme procedure has the potential to ease and enhance the engineering of phenolic acid decarboxylases.

6. LITERATURE

Anonymous 1 (2001), Joint FAO/WHO Expert Committee on Food Additives <https://apps.who.int/iris/handle/10665/42388>. Accessed on the 10th of December, 2022.

Anonymous 2 (2007), Protein Data Bank (PDB), Joint Center for Structural Genomics (JCSG) <https://www.rcsb.org/structure/2P8G> . Accessed on the 30th of November, 2021.

Abraham TE, Mathew S (2007) Ferulic Acid: An Antioxidant Found Naturally in Plant Cell Walls and Feruloyl Esterases Involved in its Release and Their Applications. *Crit Rev Biotechnol* **24**, 59-83. <https://doi.org/10.1080/07388550490491467>

Agatonovic-Kustrin S, Morton DW (2018) The Current and Potential Therapeutic Uses of Parthenolide. *Studies in Natural Products Chemistry* **58**, 61-91. <https://doi.org/10.1016/B978-0-444-64056-7.00003-9>

Akash MSH, Rehman K (2020) Essentials of Pharmaceutical Analysis. 1st Ed, Springer, Singapore, 29-56.

Alam MA, Subhan N, Hossain H, Hossain M, Reza HM, Rahman MSM, et al. (2016) Hydroxycinnamic acid derivatives: a potential class of natural compounds for the management of lipid metabolism and obesity. *Nutr Metab* **13**, 27. <https://doi.org/10.1186/s12986-016-0080-3>

Aleixandre-Tudo J, du Toit W (2018) The Role of UV-VISible Spectroscopy for Phenolic Compounds Quantification in Winemaking, in Solís-Oviedo RL, de la Cruz Pech-Canul A (eds.), *Frontiers and New Trends in the Science of Fermented Food and Beverages*, IntechOpen, London.

Alotaibi BS, Ijaz M, Buabeid M, Kharaba ZJ, Yaseen HS, Murtaza G (2021) Therapeutic Effects and Safe Uses of Plant-Derived Polyphenolic Compounds in Cardiovascular Diseases: A Review. *Drug Des Davel Ther* **15**, 4713-4732. <https://doi: 10.2147/DDDT.S327238>

Bartwal A, Mall R, Lohani P, Guru SK, Arora S (2012) Role of Secondary Metabolites and Brassinosteroids in Plant Defense Against Environmental Stresses. *J Plant Growth Regul* **32**, 216-232. <https://doi.org/10.1007/s00344-012-9272-x>

- Batish DR, Pal Singh H, Kaur S, Kohli RK, Yadav SS (2008) Caffeic acid affects early growth, and morphogenetic response of hypocotyl cuttings of mung bean (*Phaseolus aureus*). *J Plant Physiol* **165**, 297-305. <https://doi.org/10.1016/j.jplph.2007.05.003>
- Belanger JMR, Pare JRJ, Sigouin M (1997) Techniques and Instrumentation in Analytical Chemistry, Subsequent edition, Elsevier Science Ltd, Amsterdam, 37-59.
- Ben-Bassat A, Sariaslani FS, Huang LL, Patnaik R, Lowe DJ (2005) Methods for the preparation of para-hydroxycinnamic acid and cinnamic acid at alkaline pH. Patent US8003356B2
- Bernini R, Mincione E, Barontini M, Provenzano G, Setti L (2007) Obtaining 4-vinyl phenols by decarboxylation of natural 4-hydroxycinnamic acids under microwave radiation. *Tetrahedron* **63**, 9663-9667. <https://doi.org/10.1016/j.tet.2007.07.035>
- Blokker P, Boelen P, Broekman R, Rozema J (2006) The occurrence of *p*-coumaric acid and ferulic acid in fossil plant materials and their use as UV-proxy. *Plant Ecol* **182**, 197-208. https://doi.org/10.1007/978-1-4020-4445-4_13
- Boz H (2015) *p*-Coumaric acid in cereals: presence, antioxidant and antimicrobial effects. *Int J Food Sci Tech* **50**, 2323-2328. <https://doi.org/10.1111/ijfs.12898>
- Bourgaud F, Hehn A, Larbat R, Doerper S et al. (2006) Biosynthesis of coumarins in plants: a major pathway still to be unravelled for cytochrome P450 enzymes. *Phytochem Rev* **5**, 293-308. <https://doi.org/10.1007/s11101-006-9040-2>
- Brown PR (1973) High pressure liquid chromatography: Biochemical and biomedical applications. *J Chromatogr Sci*, **11**, 6-7. <https://doi.org/10.1093/chromsci/11.12.7A-b>
- Cabrita MJ, Palma V, Patao R, Costa Freitas AM (2012) Conversion of hydroxycinnamic acids into volatile phenols in a synthetic medium and in red wine by *Dekkera bruxellensis*. *Food Sci Technol* **32**, 106-111. <https://doi.org/10.1590/S0101-20612012005000024>
- Capriotti AL, Cavaliere C, Foglia P, Piovesana S, Ventura S (2014) Chromatographic Methods Coupled to Mass Spectrometry Detection for the Determination of Phenolic Acids in Plants and Fruits. *Journal of Liq Chromatog R T* **38**, 353-370. <https://doi.org/10.1080/10826076.2014.941263>

- Cavin JF, Andioc V, Etievant X, Divies C (1993) Ability of wine lactic acid bacteria to metabolize phenol carboxylic acids. *Am J Enol Vitic* **44**, 76-80. <https://doi.org/10.1111/j.1755-0238.2005.TB00285.X>
- Cavin JF, Barthelmebs L, Guzzo J, Van Beeumen J, et al. (1997) Purification and characterization of an inducible *p*-coumaric acid decarboxylase from *Lactobacillus plantarum*. *FEMS Microbiol Lett* **147**, 291-295. <https://doi.org/10.1111/j.1574-6968.1997.tb10256.x>
- Cavin JF, Dartois V, Divies C (1998) Gene Cloning, Transcriptional Analysis, Purification, and Characterization of Phenolic Acid Decarboxylase from *Bacillus subtilis*. *App Environ Microb* **64**, 1466-1471. <https://doi.org/10.1128/AEM.64.4.1466-1471.1998>
- Chen TH, Tsai MJ, Chang CS, Xu L et al. (2023) The exploration of phytochemicals theoretically combats SARS-CoV-2 pandemic against virus entry, viral replication and immune evasion. *J infect Public Health* **16**, 42-54. <https://doi.org/10.1016/j.jiph.2022.11.022>
- Cheyrier V (2012) Phenolic compounds: from plants to foods. *Phytochem Rev* **11**, 153-177. <https://doi.org/10.1007/s11101-012-9242-8>
- Cheyrier V, Rigaud J, Moutounet M (1989) High-performance liquid chromatographic determination of the free *o*-quinones of *trans*-caffeoyl tartaric acid, 2-S-glutathionylcaffeoyltartaric acid and catechin in grape must. *J Chromatogr A* **472**, 428-432. [https://doi.org/10.1016/S0021-9673\(00\)94145-1](https://doi.org/10.1016/S0021-9673(00)94145-1)
- Dai J, Mumper RJ (2010) Extraction, Analysis and Their Antioxidant and Anticancer Properties. *Molecules* **15**, 7313-7352. <https://doi.org/10.3390/molecules15107313>
- Degrassi G, Polverino de Laureto P, Bruschi CV (1995) Purification and characterization of ferulate and *p*-coumarate decarboxylase from *Bacillus pumilus*. *Appl Environ Microbiol* **64**, 326-332. <https://doi.org/10.1128/aem.61.1.326-332.1995>
- Dinakaran SK, Sujiya B, Avasarala H (2018) Profiling and determination of phenolic compounds in Indian market hepatoprotective polyherbal formulations and their comparative evaluation. *J Ayurveda Integr Med.* **9**, 3-12.
- Dziwak M, Wroblewska K, Szumny A, Galek R (2022) Modern Use of Bryophytes as a Source of Secondary Metabolites, *Agronomy* **12**, 1456. <https://doi.org/10.3390/agronomy12061456>

Edlin DAN, Narbad A, Gassib MJ, Dickinson JR, Lloyd D (1998) Purification and characterization of hydroxycinnamate decarboxylase from *Brettanomyces anomalus*. *Enzyme and Microb Tech* **22**, 232-239. [https://doi.org/10.1016/S0141-0229\(97\)00169-5](https://doi.org/10.1016/S0141-0229(97)00169-5)

El-Seedi HR, El-Said AMA, Khalifa SAM, Goransoon U, Bohlin L, Borg Karlson AK, et al. (2012) Biosynthesis, Natural Sources, Dietary Intake, Pharmacokinetic Properties, and Biological Activities of Hydroxycinnamic Acids. *J Agric Food Chem* **60**, 10877-10895. <https://doi-org.vu-nl.idm.oclc.org/10.1021/jf301807g>

Fiorini D, Caprioli G, Sagratini G, Maggi F (2014) Quantitative Profiling of Volatile and Phenolic Substances in the Wine Vernaccia di Serrapetrona by Development of an HS-SPME-GC-FID/MS Method and HPLC-MS. *Food Anal Method* **7**, 1651-1660. <https://doi.org/10.1007/s12161-014-9802-1>

Flourat AL, Combes J, Bailly-Maitre-Grand C, Magnine K, Haudrechy A, Renault JH, et al. (2020) Accessing *p*-Hydroxycinnamic Acids: Chemical Synthesis, Biomass Recovery, or Engineered Microbial Production? *Chem Sus Chem* **14**, 118-129. <https://doi.org/10.1002/cssc.202002141>

Forgasc E, Cserhati T (2003) Food Authenticity and Traceability, Woodhead Publishing, Sawston. 197-217. <https://doi.org/10.1533/9781855737181.1.197>

Franca AS, Nollet LML (2017). Spectroscopic Methods in Food Analysis (1st ed.). CRC Press, Boca Raton, 33-67. <https://doi.org/10.1201/9781315152769>

Frank A, Eborall W, Hyde R, Hart S, Turkenburg JP, Grogan G (2012) Mutational analysis of phenolic acid decarboxylase from *Bacillus subtilis* (BsPAD), which converts bio-derived phenolic acids to styrene derivatives. *Catal Sci Technol* **2**, 1568-1574. <https://doi.org/10.1039/c2cy20015e>

Galano A, Francisco-Marquez M, Alvarez-Idaboy JR (2011) Canolol: A Promising Chemical Agent against Oxidative Stress. *J Phys Chem B* **115**, 8590-8596. <https://doi.org/10.1021/jp2022105>

Gad HA, El-Ahmady SH, Abou-Shoer MI, Al-Azizi MM (2012) Application of chemometrics in authentication of herbal medicines: a review. *Phytochem Anal.* **1**, 1-24. <https://doi.org/10.1002/pca.2378>

Gloud KS (2010) Muriel Wheldale Onslow and the rediscovery of anthocyanin function in plants. In: Santos-Buelga C, Escribano-Bailon MT, Lattanzio V (eds) Recent advances in polyphenol research, 2nd ed. Blackwell, London, 206-225.

Graf E (1992) Antioxidant potential of ferulic acid. *Free Radical Bio Med* **13**, 435-448. [https://doi.org/10.1016/0891-5849\(92\)90184-I](https://doi.org/10.1016/0891-5849(92)90184-I)

Gutiérrez R, Martín del Valle EM, Galán MA (2007) Immobilized Metal-Ion Affinity Chromatography: Status and Trends, *Sep Purif Rev* **36**, 71-111. <https://doi.org/10.1080/15422110601166007>

Harnly JM, Bhaqwat S, Lin LZ (2007) Profiling methods for the determination of phenolic compounds in food and dietary supplements. *Anal Bioanal Chem* **389**, 47-61. <https://doi.org/10.1007/s00216-007-1424-7>

Hatakeyama H, Hayashi E, Haraguchi T (1977) Biodegradation of poly (3-methoxy-4-hydroxystyrene). *Polymer*, **18**. 759-763. [https://doi.org/10.1016/0032-3861\(77\)90177-X](https://doi.org/10.1016/0032-3861(77)90177-X)

He D, Shan Y, Wu Y, Liu G et al. (2011) Simultaneous determination of flavanones, hydroxycinnamic acids and alkaloid in citrus fruits by HPLC-DAD-ESI/MS. *Food Chem* **127**, 880-885. <https://doi.org/10.1016/j.foodchem.2010.12.109>

Heim KE, Tagliaferro AR, Bobilya DJ (2002) Flavonoid antioxidants: chemistry, metabolism and structure–activity relationships. *J Nutr Biochem* **13**, 572–584. [https://doi.org/10.1016/s0955-2863\(02\)00208-5](https://doi.org/10.1016/s0955-2863(02)00208-5)

Hermann BG, Blok K, Patel MK (2007) Producing bio-based bulk chemicals using industrial biotechnology saves energy and combats

Hu H, Li L, Ding S (2015) An organic solvent-tolerant phenolic acid decarboxylase from *Bacillus licheniformis* for the efficient bioconversion of hydroxycinnamic acids to vinyl phenol derivatives. *Appl Microbiol Biotechnol*, **99**, 5071–5081. <https://doi.org/10.1007/s00253-014-6313-3>

Huang WY, Cai YZ, Zhang Y (2009) Natural Phenolic Compounds from Medicinal Herbs and Dietary Plants: Potential Use for Cancer Prevention. *Nutr Cancer* **62**, 1-20. <https://doi.org/10.1080/01635580903191585>

- Iannucci A, Fragasso M, Platani C, Papa R (2013) Plant growth and phenolic compounds in the rhizosphere soil of wild oat (*Avena fatua* L.). *Front Plant Sci* **17**, 509. <https://doi.org/10.3389/fpls.2013.00509>
- Iiyama K, Lam TBT, Stone BA (1994) Covalent cross-links in the cell wall. *Plant Physiol*, **104**, 315–320. <https://doi.org/10.1104/pp.104.2.315>
- Jo S, Kim S, Shin DH, Kim MS (2020) Inhibition of SARS-CoV 3CL protease by flavonoids. *J Enzyme Inhib Med Chem* **32**, 145-151. <https://doi.org/10.1080/14756366.2019.1690480>
- Joint FAO/WHO Expert Committee on Food Additives (2001) Evaluation of certain food additives and contaminants. Fifty-fifth report of the Joint WHO/FAO Expert Committee on Food Additives. WHO Technical report series no. 901. World Health Organization, Geneva
- Jung DH, Choi W, Choi KY, Jung E, Yun H, Kazlauskas RJ, Kim BG (2013) Bioconversion of *p*-coumaric acid to *p*-hydroxystyrene using phenolic acid decarboxylase from *B. amyloliquefaciens* in biphasic reaction system. *Appl Microbiol Biotechnol* **97**, 1501-1511. <https://doi.org/10.1007/s00253-012-4358-8>
- Kabera JN, Semana E, Mussa AR, He X (2014) Plant Secondary Metabolites: Biosynthesis, Classification, Function and Pharmacological Properties. *J Pharm Pharmacol* **2**, 377-392. <https://doi.org/10.12691/jaem-5-1-4>
- Kalili KM, de Villiers A (2011) Recent developments in the HPLC separation of phenolic compounds. *J Sep Sci* **34**, 854-897. <https://analyticalsciencejournals.onlinelibrary.wiley.com/doi/full/10.1002/jssc.201000811>
- Karmakar B, Vohra RM, Nandanwar H, Sharma P, Gupta KG, Sobti RC (2000) Rapid degradation of ferulic acid via 4-vinylguaiacol and vanillin by a newly isolated strain of *Bacillus coagulans*. *J Biotechnol* **80**,195-202. [https://doi.org/10.1016/S0168-1656\(00\)00248-0](https://doi.org/10.1016/S0168-1656(00)00248-0)
- Kilic I, Yesiloglu Y (2013) Spectroscopic studies on the antioxidant activity of *p*-coumaric acid. *Spectrochimica Acta Part A. Adv Chem Ser* **115**, 719-724. <https://doi.org/10.1016/j.saa.2013.06.110>

- Koshihara Y, Neichi T, Murota SI, Lao AN, Fujimoto Y, Tatsuno T (1984) Caffeic acid is a selective inhibitor for leukotriene biosynthesis. *Biochem Biophys Acta* **792**, 92-97. [https://doi.org/10.1016/0005-2760\(84\)90287-X](https://doi.org/10.1016/0005-2760(84)90287-X)
- Koseki T, Ito Y, Furuse S, Ito K, Iwano K (1996) Conversion of ferulic acid into 4-vinyl guaiacol, vanillin and vanillic acid in model solutions of shochu. *J Ferment Bioeng*, **82**, 46-50. [https://doi.org/10.1016/0922-338X\(96\)89453-0](https://doi.org/10.1016/0922-338X(96)89453-0)
- Koski A, Pekkarinen S, Hopia A, Waehaelae K, Heinonen M (2003) Processing of rapeseed oil: effects on sinapic acid derivate content and oxidative stability. *Eur Food Res Technol* **217**, 110-114. <https://doi.org/10.1007/s00217-003-0721-4>
- Krygier K, Sosulski F, Hogge L (1982) Free, esterified, and insoluble-bound phenolic acids. 1. Extraction and purification procedure. *J Agric Food Chem* **30**, 330-334. <https://doi.org/10.1021/jf00110a028>
- Kuppusamy P, Kim D, Park HS, Jung JS et al. (2020) Quantitative Determination of Phenolic Acids and Flavonoids in Fresh Whole Crop Rice, Silage, and Hay at Different Harvest Periods. *Appl Sci* **10**, 7981. <https://doi.org/10.3390/app1022798>
- Lall RK, Syed DN, Adhami VM, Khan MI, Mukhtar H (2015) Dietary Polyphenols in Prevention and Treatment of Prostate Cancer. *Int J Mol Sci* **16**, 3350-3376. <https://doi.org/10.3390/ijms16023350>
- Landete JM, Rodríguez H, Curiel JA, de las Rivas B, Mancheño JM, Muñoz R (2010) Gene cloning, expression, and characterization of phenolic acid decarboxylase from *Lactobacillus brevis* RM84, *J Ind Microbiol Biotechnol*, **37**, 617–624. <https://doi.org/10.1007/s10295-010-0709-6>
- Lattanzio V (2013) Phenolic Compounds: Introduction. In: Ramawat KG, Merillon JM (eds.) *Natural Products*. Springer, Berlin 1543-1580. https://doi.org/10.1007/978-3-642-22144-6_57
- Lee IY, Volm TG, Rosazza JPN (1998) Decarboxylation of ferulic acid to 4-vinylguaiacol by *Bacillus pumilus* in aqueous-organic solvent two-phase systems. *Enzyme Microb Technol* **23**, 261-266. [https://doi.org/10.1016/S0141-0229\(98\)00044-1](https://doi.org/10.1016/S0141-0229(98)00044-1)

- Leibig D, Muller AHE, Frey H (2016) Anionic Polymerization of Vinyl catechol Derivates: Reversal of the Monomer Gradient Directed by the Position of the Catechol Moiety in the Copolymerization with Styrene. *Macromolecules* **49**, 4792-4801. <https://doi.org/10.1021/acs.macromol.6b00831>
- Li AN, Li S, Zhang YJ, Xu XR, Chen YN, Li HB (2014) Resources and Biological Activities of Natural Polyphenols. *Nutrients*. **6**, 6020-6047. <https://doi.org/10.3390/nu6126020>
- Li Y, Peng Q, Selimi D, Wang Q, Charkowski AO, Chen X, et al. (2009) The plant Phenolic Compound *p*-Coumaric Acid Represses Gene Expression in the *Dickeya dadantii* Type III Secretion System. *Appl Environ Microbiol* **75**, 1223-1228. <https://doi.org/10.1128/AEM.02015-08>
- Li Q, Ying X, Zho T, Gong Y et al. (2021) Improving the catalytic characteristic of phenolic acid decarboxylase from *Bacillus amyloliquefaciens* by the engineering of N-terminus and C-terminus. *BMC Biotechnol* **21**, 44. <https://doi.org/10.1186/s12896-021-00705-7>
- Liang XW, Dron M, Cramer CL, Dixon RA, Lamb CJ (1989) Differential regulation of phenylalanine ammonia-lyase genes during plant development and by environmental cues. *J Biol Chem* **264**, 14486-14492. [https://doi.org/10.1016/S0021-9258\(18\)71704-3](https://doi.org/10.1016/S0021-9258(18)71704-3)
- Lin CW, Tsai FJ, Tsai CH, Lai CC, Wan L, Ho TY, et al. (2005) Anti-SARS coronavirus 3C-like protease effects of *Isatis indigotica* rppt and plant derived phenolic compounds. *Antivir Res* **68**, 36-42. <https://doi.org/10.1016/j.antiviral.2005.07.002>
- Maeda HA (2019) Evolutionary Diversification of Primary Metabolism and Its Contribution to Plant Chemical Diversity. *Front Plant Sci* **10**, 881. <https://doi.org/10.3389/fpls.2019.00881>
- Marchiosi R, Dantas dos Santos W, Constantin RP, Barbarosa de Lima R, Soares AR, et al. (2020) Biosynthesis and metabolic actions of simple phenolic acids in plants. *Phytochem Rev* **19**, 865-906. <https://doi.org/10.1007/s11101-020-09689-2>
- Mathew S, Abraham TE (2006) Bioconversion of ferulic acid a hydroxycinnamic acid. *Crit Rev Microbiol*, **32**. 115-125. <https://doi.org/10.1080/10408410600709628>

- Merecz-Sadowska A, Sitarek P, Kucharska E, Kowalczyk T, Zajdel K, Ceglinski T, et al. (2021) Antioxidant Properties of Plant-Derived Phenolic Compounds and Their effect on Skin Fibroblast Cells. *Antioxidans* **10**. 726. <https://doi.org/10.3390/antiox10050726>
- Mishra S, Sachan A, Vidyarathi AS, Sachan SG (2014) Transformation of ferulic acid to 4-vinyl guaiacol as major metabolite: a microbial approach. *Rev in Environ Sci and Biotechnol* **13**, 377-385. <https://doi.org/10.1007/s11157-014-9348-0>
- Mittmann E, Gallus S, Bitterwolf; Oelschlaeger C (2019) A phenolic Acid Decarboxylase-Based All-Enzyme Hydrogel for Flow Reactor Technology. *Micromachines-Basel* **10**. 795. <https://doi.org/10.3390/mi10120795>
- Miyagusuku-Cruzado G, Garcia-Cano I, Rocha-Mendoza D, Jimenez-Flores R, Giusti MM (2020) Monitoring Hydroxycinnamic Acid Decarboxylation by Lactic Acid Bacteria Using High-Throughput UV-Vis Spectroscopy. *Molecules*, **25**. 3142. <https://doi.org/10.3390/molecules25143142>
- Mojzer EB, Hrnčić MK, Škerget M, Knez Ž, Bren U (2016) Polyphenols: Extraction, Methods, Antioxidative Action, Bioavailability and Anticancerogenic Effects. *Molecules* **21**, 901. <https://doi.org/10.3390/molecules21070901>
- Mondal A, Gandhi A, Fimognari C, Atanasov AG, Bishayee A (2019) Alkaloids for cancer prevention and therapy: Current progress and future perspectives. *Eur J Pharmacol* **5**, 172472. <https://doi.org/10.1016/j.ejphar.2019.172472>
- Morley KL, Grosse S, Leisch H, Lau PCK (2013) Antioxidant Canolol Production from a Renewable Feedstock via an Engineered Decarboxylase. *Green Chem* **15**, 3312-3317. <https://doi.org/10.1039/c3gc40748a>
- Muhamadejev R, Melngaile R, Paegle P, Zibarte I, Petrova M, Jaudzems K, et al. (2021) Residual Solvent Signal of CDCl₃ as a qNMR Internal Standard for Application in Organic Chemistry Laboratory. *J Org Chem* **86**, 3890-3896. <https://doi.org/10.1021/acs.joc.0c02744>
- Ncube B, Ndhala AR, Van Staden J (2017) Secondary Metabolism and the Rationale for Systems Manipulation. In: Jha S (eds) *Transgenesis and Secondary Metabolism*, Reference Series in Phytochemistry. Springer, Cham, 45-65. <https://doi.org/10.1016/j.jaim.2016.12.006>

- Nićiforović N, Abramović H (2013) Sinapic Acid and Its Derivates: Natural Sources and Bioactivity. *Compr Rev Food Sci F* **13**, 34-51. <https://doi-org.vu-nl.idm.oclc.org/10.1111/1541-4337.12041>
- Nilapwar SM, Nardelli M, Westerhoff Hv, Verma M (2011) Absorbtion Spectroscopy, *Methods Enzymol*, **500**, 59-75. <https://doi.org/10.1016/B978-0-12-385118-5.00004-9>
- Nishimori K, Tenjimbayashi, Naito M, Ouchi M (2020) Alternating Copolymers of Vinyl Catechol of Vinyl Phenol with Alkyl Maleimide for Adhesive and Water-Repellent Coating Materials. *ACS Appl Polym Mater* **2**, 4604-4612. <https://doi.org/10.1021/acsapm.0c00682>
- Noda S, Kawai Y, Tanaka T, Kondo A (2014) 4-Vinylphenol biosynthesis from cellulose as the sole carbon source using phenolic acid decarboxylase- and tyrosine ammonia lyase-expressing *Streptomyces lividans*. *Bioresour Technol* **180**, 59-65. <https://doi.org/10.1016/j.biortech.2014.12.064>
- Novaković L, Guo T, Bacic A, Sampathkumar A, Johnson KL (2018) Hitting the Wall-Sensing and Signaling Pathways Involved in Plant Cell Wall Remodeling in Response to Abiotic Stress. *Plants* **7**, 89. <https://doi:10.3390/plants7040089www.mdpi.com/journal/plants>
- de Olivera DM, Finger-Teixeira A, Rodrigues Mota T, Salvador VH, Moreira-Vilar FC, Correa Molinari HB et al. (2015) Ferulic acid: a key component in grass lignocellulose recalcitrance to hydrolysis. *Plant Biotechnol J* **13**, 1224-1232. <https://doi.org/10.1111/pbi.12292>
- Olthof MR, Hollman PCH, Katan M (2001) Chlorogenic acid and caffeic acid are absorbed in humans. *Hum Nutr Metabol* **131**, 66-71. <https://doi.org/10.1093/jn/131.1.66>
- Payer SE, Sheng X, Pollak H, Wuensch C, et al. (2017) exploring the Catalytic Promiscuity of Phenolic Acid Decarboxylases: Asymmetric, 1,6-Conjugate Addition of Nucleophiles Across 4-Hydroxystyrene. *Adv Synth Catal* **359**, 2066-2075. <https://doi.org/10.1002/adsc.201700247>
- Pichersky E, Gang DR (2000) Genetics and biochemistry of secondary metabolites in plants: an evolutionary perspective. *Trends Plant Sci* **5**, 439-445. [https://doi.org/10.1016/S1360-1385\(00\)01741-6](https://doi.org/10.1016/S1360-1385(00)01741-6)
- Priefert H, Rabenhorst J, Steinbüchel A (2001) Biotechnological production of vanillin. *Appl Microbiol Biotechnol*, **56**, 296–314. <https://doi.org/10.1007/s002530100687>

Pyrzynska K, Sentkowska A (2015) Recent Developments in the HPLC Separation of Phenolic Food Compounds. *Crit Rev Anal Chem* **45**, 41-51. <https://doi-org.vu-nl.idm.oclc.org/10.1080/10408347.2013.870027>

Qu YC, Wang Z, Lu Q, Zhang Y (2013) Selective Production of 4-Vinylphenol by Fast Pyrolysis of Herbaceous Biomass. *Ind Engineer Chem* **52**, 12771-12776. <https://doi.org/10.1021/ie401626d>

Rasouli H, Hosseini-Ghazvini SMB, Adibi H, Khodarahmi R (2017) Differential α -amylase/ α -glucosidase inhibitory activities of plant-derived phenolic compounds: a virtual screening perspective for the treatment of obesity and diabetes. *Food Funct* **8**, 1942-1954. <https://doi:10.1039/C7FO00220C>

Ren X, Li X, Yin L, Jiang D, Hu D (2020) Design, Synthesis, Antiviral Bioactivity, and Mechanism of the Ferulic Acid Ester-Containing Sulfonamide Moiety. *ACS Omega* **5**, 19721-19726. <https://doi.org/10.1021/acsomega.0c02421>

Robbins RJ (2003) Phenolic acids in foods: an overview of analytical methodology. *J Agric Food Chem* **51**, 2866-2887. <https://doi.org/10.1021/jf026182t>

Rocha FS, Gomes AJ, Lunardi CN, Kaliaguine S, Patience GS (2018) Experimental Methods in Chemical Engineering: Ultraviolet Visible Spectroscopy – UV-VIS. *J Chem Engineer* **96**, 2512-2517. <https://doi.org/10.1002/cjce.23344>

Rodriguez H, Landete JM, Curiel JA, Rivas B, Mancheno JM, Munoz R (2008) Characterization of the *p*-coumaric acid decarboxylase from *Lactobacillus plantarum* CECT 748(T). *J Agric Food Chem* **56**, 3068-3072.

Rosazza JPN, Huang Z, Dostal L, Volm T & Rousseau B (1995) Review: Biocatalytic transformations of ferulic acid: an abundant aromatic natural product. *J Ind Microbiol*, **15**, 457–471. <https://doi.org/10.1007/BF01570016>

Schwab W (2003) Metabolome diversity: too few genes, too many metabolites? *Phytochemistry* **62**, 837-849. [https://doi:10.1016/S0031-9422\(02\)00723-9](https://doi:10.1016/S0031-9422(02)00723-9)

Schweiger AK, Rios-Lombardia N, Winkler CK, Schmidt S, Moris F, Kroutil W, et al. (2019) Using Deep Eutectic Solvents to Overcome Limited Substrate Solubility in the Enzymatic

Decarboxylation of Bio-Based Phenolic Acids. *ACS Sustainable Chem Eng*, **7**, 16364-16370. <https://doi.org/10.1021/acssuschemeng.9b03455>

Serra S, Fuganti C, Brenna E (2005) Biocatalytic preparation of natural flavours and fragrances. *Trends Biotechnol*, **23**, 193-198. <https://doi.org/10.1016/j.tibtech.2005.02.003>

Sherma J (2003) Handbook of thin-layer chromatography. Chromatographic Science Series. *J Nat Prod*, **89**, 1199. <https://doi.org/10.1021/np030741o>

Stalikas CD (2007) Extraction, separation, and detection methods for phenolic acids and flavonoids. *J Sep Sci*, **30**, 3268-3295. <https://doi.org/10.1002/jssc.200700261>

Stojković D, Soković J, Glamoclija M, Kukić-Marković M, Petrović Silvana S (2013) In situ antioxidant and antimicrobial activities of naturally occurring caffeic acid, *p*-coumaric acid and rutin, using food systems. *J Sci Food Agric* **93**, 3205-3208. DOI: 10.1002/jsfa.6156

Suleymanova F, Nesterova O, Matyushin A (2019) HPLC Quantification of Hydroxycinnamic and Organic Acids of Canadian Goldenrod (*Solidago canadensis L.*). *Pharmacogn Mag* **11**, 400-404. <https://org.doi/10.5530/pj.2019.11.62>

Takeshima H, Satoh K, Kamigaito M (2018) Scalable Synthesis of Bio-Based Functional Styrene: Protected Vinyl Catechol from Caffeic Acid and Controlled Radical and Anionic Polymerizations Thereof. *ACS Sustainable Chem Eng* **6**, 13681-13686. <https://doi.org/10.1021/acssuschemeng.8b04400>

Tarrant AWS (2010) Instrumentation Reference Book, 4th ed., Butterworth-Heinemann, Oxford, 499-519. <https://doi.org/10.1016/B978-0-7506-8308-1.00028-0>

Torre-Carbot K, Jauregui O, Gimeno E, Castellote AI (2005) Characterization and Quantification of Phenolic Compounds in Olive Oils by Solid-Phase Extraction, HPLC-DAD, and HPLC-MS/MS. *J Agr Food Chem* **53**, 4331-4340. <https://doi.org/10.1021/jf0501948>

Torres J, Rosazza JPN (2001) Microbial transformations of *p*-coumaric acid by *Bacillus megaterium* and *Curvularia lunata*. *Journal of Natural Products* **64**, 1408-1414. <https://doi.org/10.1021/np010238g>

Tomohara K, Adachi I, Horino Y, Kesamaru H, Abe H, Suyama K, et al. (2019) DMSO-Perturbing Assay for Identifying Promiscuous Enzyme Inhibitors, *ACS Med Chem Lett.* **10**, 923-928. <https://doi.org/10.1021/acsmchemlett.9b00093>

Tran NP, Gury J, Dartois V, Nguyen TKC, Seraut H, Barthelmebs B, et al. (2008) Phenolic Acid-Mediated Regulation of the padC Gene, Encoding the Phenolic Acid Decarboxylase of *Bacillus subtilis*. *J Bacteriol*, **190**, 3213-3224. <https://doi.org/10.1128/JB.01936-0>

Tsao R (2010) Chemistry and biochemistry of dietary polyphenols. *Nutrients*, **2**, 1231-1246. <https://doi.org/10.3390/nu2121231>

Tzima K, Brunton NP, Rai DK (2018) Qualitative and Quantitative Analysis of Polyphenols in Lamiaceae Plants – A Review. *Plants*, **2**, 25. <https://doi.org/10.3390/plants7020025>

van Beek S, Priest FG (2000) Decarboxylation of substituted cinnamic acids by lactic acid bacteria isolated during malt whisky fermentation. *Appl Environ Microbiol* **66**, 5322-5328. <https://doi.org/10.1128/AEM.66.12.5322-5328.2000>

Vanbeneden N, Gils F, Delavaux F, Delvaux FR (2008) Formation of 4-vinyl and 4-ethyl derivatives from hydroxycinnamic acids: Occurrence of volatile phenolic flavor compounds in beer and distribution of Pad1-activity among brewing yeast. *Food Chem*, **107**, 221-230. <https://doi.org/10.1016/j.foodchem.2007.08.008>

Williamson JJ, Bahrin N, Hardiman EM, Bugg TDH (2020) Production of Substituted Styrene Bioproducts from Lignin and Lignocellulose Using Engineered *Pseudomonas putida* KT2440. *Biotechnol J* **15**, 1900571. <https://doi.org/10.1002/biot.201900571>

Wu S, Chappell J (2008) Metabolic engineering of natural products in plants; tools of the trade and challenges for the future. *Curr Opin Biotechnol*, **19**, 145–152. <https://doi.org/10.1016/j.copbio.2008.02.007>

Wuensch C, Gross J, Steinkellner G, Gruber K, Glueck SM, Faber K (2013) Asymmetric enzymatic hydration of hydroxystyrene derivatives. *Angew Chem Int Ed*, **52**, 2293–2297. <https://doi.org/10.1002/anie.201207916>

- Wuensch C, Pavkov-Keller T, Steinkellner G, Gross J, Fuchs M, Hromic A, et al. (2015) Regioselective enzymatic β -carboxylation of para-hydroxystyrene derivatives catalyzed by phenolic acid decarboxylases. *Adv Synth Catal*, **357**, 1909–1918. <https://doi.org/10.1002/adsc.201401028>
- Xu H, Zhao S, Xiong X, Yao J, Cross RJ, Saunders M (2017) Deuterated Ethanol as a Probe for Measuring Equilibrium Isotope Effects for Hydroxyl Exchange, *J Phys Chem A*, **121**. 2288-2292. <https://doi.org/10.1021/acs.jpca.7b00514>
- Yang J, Sun XQ, Yan SY, Pan WJ, Zhang MX, Cai QN (2017) Interaction of Ferulic Acid with Glutathione S-Transferase and Carboxylesterase Genes in the Brown Planthopper, *Nilaparvata lugens*. *J Chem Ecol* **43**, 693-702. <https://doi.org/10.1007/s10886-017-0859-3>
- Zago E, Dubreucq E, Lecomte J, Villeneuve P, Fine F, Fulcrand H (2016) Synthesis of bio-based epoxy monomers from natural allyl- and vinyl phenols and the estimation of their affinity to the estrogen receptor α by molecular docking. *New J Chem* **40**, 7701-7710. <https://doi.org/10.1039/c6nj00782a>
- Zaldivar J, Ingram LO (1999) Effect of organic acids on the growth and fermentation of ethanologenic *Escherichia coli* LY01. *Biotechnol Bioeng*, **66**, 203–210. [https://doi.org/10.1002/\(sici\)1097-0290\(1999\)66:4<203::aid-bit1>3.0.co;2-#](https://doi.org/10.1002/(sici)1097-0290(1999)66:4<203::aid-bit1>3.0.co;2-#)
- Zhao N, Wang G, Norris A, Chen X et al. (2013) Studying Plant Secondary Metabolism in the Age of Genomics. *Crit Rev Plant Sci* **32**, 369-382. <https://doi.org/10.1080/07352689.2013.789648>
- Zuo Y, Wang C, Zhan J (2002) Separation, Characterization, and Quantitation of Benzoic and Phenolic Antioxidants in American Cranberry Fruit by GC-MS. *J Agric Food Chem* **50**, 3789-3794. <https://doi.org/10.1021/jf020055f>
- Zhou Q, Qian Y, Qian MC (2015) Analysis of volatile phenols in alcoholic beverage by ethylene glycol-polydimethylsiloxane based stir bar sorptive extraction and gas chromatography-mass spectrometry. *J Chromatogr A* **1390**, 22-27. <https://doi.org/10.1016/j.chroma.2015.02.064>
- Zheng L, Sun Z, Bai Y, Wang J, Guo X (2007) Production of vanillin from waste residue of rice bran oil by *Aspergillus niger* and *Pycnoporus cinnabarinus*. *Bioresource Technol*, **98**. 1115-1119. <https://doi.org/10.1016/j.biortech.2006.03.028>

LIST OF ABBREVIATIONS

^1H NMR	Proton nuclear magnetic resonance
4-VC	4-Vinyl catechol
4-VG	4-Vinyl guaiacol
4-VP	4-Vinyl phenol
4-VS	4-Vinyl syringol
ACN	Acetonitrile
Arg	Arginine
BCA	Bicinchoninc acid assay
<i>Bs</i> PAD	Phenolic acid decarboxylase from <i>Bacillus subtilis</i>
<i>Bs</i> PAD_wt	Phenolic acid decarboxylase from <i>Bacillus subtilis</i> wild type
<i>Bs</i> PAD_I85A	Phenolic acid decarboxylase from <i>Bacillus subtilis</i> I85A mutant
BW	Buffer wash
CAA	Caffeic acid
CDCl_3	Deuterated chloroform
CFE	Cell free extract
<i>p</i> -CUA	<i>p</i> -Coumaric acid
CV	Column volume
DAD	Diode-array detector

ddH ₂ O	Double-distilled water
DMSO	Dimethyl sulfoxide
FA	Ferulic acid
FAD	Ferulic acid decarboxylase
FID	Flame-ionisation detector
FPD	Flame photometric detector
FT	Flow through
GC	Gas-chromatography
Glu	Glutamate
HPLC	High-performance liquid chromatography
HOMO	Highest occupied molecular orbit
IMBT	Institute of Molecular Biotechnology
IPTG	Isopropyl β-D-1-thiogalactopyranosid
KPi	Potassium-phosphate buffer
LB	Lysogeny Broth
LC	Liquid chromatography
LDS	Lithium dodecyl sulphate
LUMO	Lowest unoccupied molecular orbit
MBTE	Methyl tert-butyl ether
MES	2-(N-morpholino)ethanesulfonic acid
MS	Mass spectrometry
NMR	Nuclear magnetic resonance

NPD	Nitrogen-phosphorus detector
ONC	Over-night culture
PAD	Phenolic acid decarboxylase
PAL	Phenylalanine ammonia-lyase
PDC	<i>p</i> -Coumaric acid decarboxylase
PVS	Polyvinylsyringol
SA	Sinapic acid
SDS-PAGE	Sodium dodecyl sulphate polyacrylamide gel electrophoresis
TAL	Tyrosine ammonia-lyase
TB	Terrific broth
TCD	Thermal conductivity detector
TLC	Thin layer chromatography
TRIS	Tris (hydroxymethyl) aminomethane
Tyr	Tyrosine
UV	Ultraviolet
UV-VIS	Ultraviolet-visible

DECLARATION OF ORIGINALITY

I MIRNA LARVA declare that this master thesis is an original result of my own work and it has been generated by me using no other resources than the ones listed in it.

A handwritten signature in black ink, appearing to read 'Larva', is written above a horizontal line.

Signature